Surface Chemistry of Prototypical Bulk II–VI and III–V Semiconductors and Implications for Chemical Sensing

Fazila Seker,[†] Kathleen Meeker,[†] Thomas F. Kuech,[‡] and Arthur B. Ellis*[,†]

Departments of Chemistry and Chemical Engineering, University of Wisconsin—Madison, Madison, Wisconsin 53706

Received September 20, 1999

Contents

I. Introduction

Bulk II−VI and III−V single-crystal semiconductors provide an appealing coupling of chemical, electrical, and optical properties that can be exploited in the design of chemical sensors. The surfaces of these materials provide chemically and physically diverse binding platforms for gaseous and solution analytes. Over the past 20 years, many studies have indicated that the rich coordination chemistry of the substrate surface can be used to influence the electrooptical properties of the semiconductor.[1] In this way, transduction of a chemical binding event on the surface into an electrical or optical signal is possible and can serve as the basis for sensor design. Elucidation of the relationship between the surface chemistry of the binding event and its effect on the electronic structure and properties of the semiconductor substrate is a fundamental issue in surface science and chemical sensing. While UHV studies have provided considerable insight into this relationship for some semiconductors, chemical sensing is typically conducted under far less stringent experimental conditions, where the inability to predict these chemical−electronic relationships currently limits use of II−VI and III−V materials for analyte detection.

There is considerable promise, however, for the use of semiconductor substrates for chemical sensing. The diversity in II−VI and III−V chemical, structural, and electronic surface composition provides many opportunities for creating surfaces with tailored physicochemical properties and for tuning the electronic properties of the underlying bulk semiconductor material, for detection of a target analyte. The spatially localized electronic states that characterize semiconductor surfaces, surface states, pose a barrier to surface migration of adsorbed species.[2] Consequently, site-specific adsorption of molecules typically occurs. For example, in the case of GaAs, the prototypical III−V semiconductor, a molecule can bind to

[†] Department of Chemistry.
[‡] Department of Chemical Engineering.

10.1021/cr980093r CCC: $35.00
Published on Web 06/09/2000

A native Canadian, Fazila Seker received her B.Sc. degree from the University of Toronto in 1994 and completed her doctoral work with an emphasis on polymer/semiconductor interfaces with Arthur B. Ellis in the summer of 1999. She is currently a research scientist at the Polymer Materials Laboratory at the General Electric Corporate Research and Development Center.

Thomas F. Kuech is the Milton J. and A. Maude Shoemaker Professor of Chemical Engineering at the University of Wisconsin—Madison. His research interests are in solid-state materials properties and semiconductor processing, particularly involving chemical vapor deposition methods. He directs the National Science Foundation's Materials Research Science and Engineering Center on Nanostructured Materials and Interfaces.

After receiving her bachelor's degree from Oberlin College, Kathleen Meeker began research with Arthur B. Ellis on semiconductor-based chemical sensors and received her doctoral degree in the summer of 1999. She is currently studying the photophysical properties of conjugated polymers with applications in light-emitting diodes as a postdoctoral researcher with Professor Samson A. Jenekhe at the University of Rochester.

Arthur B. Ellis is the Meloche-Bascom Professor of Chemistry at the University of Wisconsin—Madison. His research group investigates the electrooptical properties of solids, including tailoring semiconductor surfaces for use as chemical sensing platforms. He is also involved in education projects designed to incorporate current research in materials science into science and engineering curricula.

the surface via exposed surface Ga or surface As atoms. The crystal's orientation and conductivity are also important parameters that can affect adsorption. In the case of CdS, for example, the wurtzite structure of the solid can be oriented so that a polar Cd-rich (0001) or S-rich ($000\bar{1}$) or nonpolar ($11\bar{2}0$) face can be used for adsorption. Semiconductors such as CdTe and GaAs can be either n- or p-type, allowing optimization of sensor characteristics.

Creating sensors from II−VI and III−V materials requires chemical control of substrate properties for optimizing such sensor characteristics as selectivity, sensitivity, speed of response, and durability. Analyte detection is attributed to perturbation of the electrooptical properties of the semiconductor through analyte-induced changes in the band bending and/or surface recombination velocity.[1] If these changes are detectable and reversible, reflecting weak chemisorption, on-line detection is possible. Permanent changes arising from irreversible reactions can be useful in designing dosimeters for chemical analysis, as well as for the preparation of designer semiconductor surfaces. Chemisorption may cause no detectable change in the electronic properties of the substrate; in such a case, tailored modification of semiconductor surface properties is an exciting emerging technology, which can be used to extend the semiconductor's sensitivity to these otherwise inert analytes.

A sense of how the electronic structure of the substrate can lead to such disparate properties has developed through an understanding of surface states. At one extreme, a semiconductor might possess a high density of surface states that pins its Fermi level near mid-gap, making it resistant to adsorbate-induced perturbation of electronic properties, and therefore, precluding adsorbate detection. In contrast to such a pinned system, a distribution of surface states that is substantially perturbed by interaction with adsorbate orbitals can lead to reversible or irreversible changes in electrooptical properties and allow real-time or integrated sensing to occur, respectively.

The principal objective of this review is to clarify, insofar as possible, the effects of various surface

treatments on the chemical reactivity of prototypical II−VI and III−V semiconductor surfaces and how the physicochemical properties of these surfaces are linked to the electrooptical properties of the semiconductors to make signal transduction possible. It is common, for example, to etch II−VI and III−V semiconductors, and considerable empirical literature is available on the dependence of etch rate on such parameters as crystal orientation and etchant composition and temperature. Similarly, films have been applied to these materials by methods as simple as dip coating. Surface preparations based on site-selective chemistry with particular surface atoms of II−VI and III−V materials have been studied. While the chemical composition and physical structure of the resulting surfaces have typically been difficult to determine, a variety of new experimental tools have appeared over the past two decades that are sharpening our understanding of the effects of these surface treatments. Likewise, we have better tools for examining how surface treatments are affecting the electronic structure of the treated solids.

This review article will summarize these issues associated with chemical sensing using single-crystal semiconductor substrates. Related summaries of nanoparticulate semiconductor sensor structures have been published.[3] There is a voluminous body of literature related to the surface properties of III−V semiconductors, particularly GaAs, and recent summaries are available.[4−8] We will focus in this review on a subset of the literature that is most directly applicable to sensor design and in particular to the use of semiconductor photoluminescence (PL) as a method for analyte detection, as PL has been used to characterize a particularly wide range of analyte−II−VI and analyte−III−V interactions. Many of the principles discussed herein are, however, applicable to other transduction mechanisms, such as detection through electrical methods.

The organization of this review article begins with background information on the effects of adsorbates on the electronic structure of semiconductors. This is followed by a section on techniques used to characterize the adsorbate-coated semiconductor surfaces, with regard to the chemical, physical, and electronic structure of the semiconductor substrate. Various surface modification techniques and their effects on the semiconductor's electronic properties comprise the succeeding sections. Some issues related to sensor implementation are then discussed in a concluding section.

II. The Electronic Structure of Semiconductors and the Effects of Adsorption: Transduction Mechanisms in Analyte Detection

A. Overview of Semiconductor Electronic Structure

This section provides an overview of the electronic structure of semiconductors necessary for understanding the origin of the transduction mechanism and ultimately for designing strategies for optimizing sensor response characteristics. Figure 1 summarizes

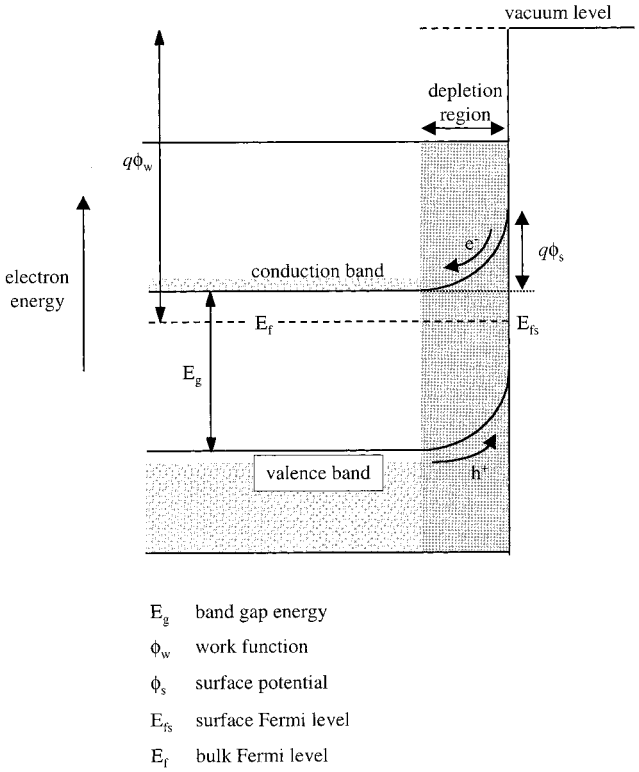

Figure 1. Diagram illustrating the electronic structure of a semiconductor, with the vertical right-hand line indicating the surface of the solid. Shown in the diagram for an n-type semiconductor are the band gap, E_g, work function, ϕ_w, bulk Fermi level, E_f, surface Fermi level, E_{fs}, and surface potential, ϕ_s. The near-surface electric field, the depletion region, is shaded, and the filled electronic levels are speckled.

general features of a semiconductor's electronic structure for an n-type material in which the majority of the charge carriers are electrons. The valence band and conduction band are separated by a band gap energy, E_g, that characterizes the strength of the bonding interactions between the atoms comprising the sample. For the III−V and II−VI semiconductors of interest, E_g lies in the visible to near-IR part of the spectrum. In an ideal crystal there are no electronic states within the range of energies corresponding to the band gap.[9]

The energetic distribution of charge carriers in the solid is given by the Fermi−Dirac distribution function (eqs 1a and b), which specifies the Fermi level, E_f, as the energy at which the electron and hole reside with equal probability

$$f(e^-) = 1/[1 + g\ \exp((E - E_f)/k_b T)] \qquad (1a)$$

$$f(h^+) = 1/[1 + g\ \exp((E_f - E)/k_b T)] \qquad (1b)$$

where $f(e^-)$ and $f(h^+)$ are the probabilities corresponding to electron or hole occupation, respectively, of a given electronic state at energy E having a degeneracy of g; k_b and T are the Boltzmann constant and absolute temperature, respectively.[10] The Fermi level defines the electrochemical potential of a system, with all states below E_f mostly occupied with electrons and all states above it mostly empty. The minimum energy required to extract an electron from

the Fermi level at the surface of the solid, E_{fs}, to the vacuum level can be measured and defines the work function, ϕ_w. The work function has been considered to be analogous to the electronegativity in molecular systems.[11−13]

Localized surface states within the gap often occur with II−VI and III−V materials and can lead to a near-surface electric field in the solid, represented by the bending of the bands at the surface in Figure 1, and a surface potential ϕ_s. The origin and importance of these localized states are the subject of the next section.

B. Analyte Binding: Surface States and Orbital Considerations

The coordinative unsaturation of many II−VI and III−V semiconductor surface atoms relative to their bulk counterparts can lead to electronic states that are both spatially and energetically localized.[9,14] Wave functions corresponding to surface states have a maximum value at the surface, and they decay exponentially away from the surface to the regions both inside and outside the semiconductor bulk. When these surface states have energies within the band gap, they can have a great impact on semiconductor electronic properties and adsorption processes, with important consequences for analyte detection.

Surface states can be either intrinsic or extrinsic in origin. Intrinsic surface states arise naturally from solutions to the Schrödinger equation by imposing boundary conditions to reflect the aperiodic termination of the lattice at the surface. Defects owing to surface reconstruction are also termed intrinsic. Theoretical studies suggest that by occupying vacant coordination sites of surface atoms, adsorbates can induce surface atoms to adopt near-bulk coordination geometries; in some cases, this may even lead to removal of intrinsic surface states.[15−18] In contrast, extrinsic surface states are new states introduced by foreign adsorbed material. These new states correspond to dangling bonds of the adsorbate, which energetically may lie within the band gap or overlap with continuum bulk states. Oxide formation at the semiconductor surface, for example, is a common source of extrinsic surface states.

Holes or electrons can become trapped at surface states to create a localized charge layer at the surface, giving rise to an electrostatic field in the near-surface region within the semiconductor, as illustrated in Figure 1. The degree of band bending is quantified by the surface potential, ϕ_s. It is also commonly described by the *surface* Fermi level, denoted as E_{fs}, which is usually specified relative to the band edges. The width of this electric field region, the depletion width, plays a critical role in carrier dynamics.[9,19] Modification of the energetic distribution and/or the surface density of states (SDOS) by adsorption can sometimes shift the energetic position of E_{fs} relative to the band edges, perturbing the electric field and giving rise to measurable changes in electrical and optical properties.

This adsorbate-induced perturbation of electronic structure can be understood on the basis of molecular orbital interactions between the frontier orbitals of the adsorbing analyte and semiconductor surface atoms.[14] In discussing adsorbate interactions with the surface, it is convenient to categorize adsorbates as donors, D, or acceptors, A, which, by definition, can react in the following way with the semiconductor surface during adsorption:[10]

$$D \rightarrow D^+ + e^- \quad (2a)$$

$$A + e^- \rightarrow A^- \quad (2b)$$

The orbital interactions for donor and acceptor adsorbates binding to the surface are illustrated in Figure 2 for both n- and p-doped cases. Binding of a donor (Figure 2a) occurs if it has a HOMO (highest occupied molecular orbital) that energetically lies close to a vacant semiconductor surface state and satisfies the symmetry requirements for combining with the surface orbital; such an interaction enables donation of electron density to the semiconductor. Similarly, acceptor binding (Figure 2b) relies on the availability of a low-lying LUMO (lowest unoccupied molecular orbital) that can combine with a filled surface state, thereby accepting electron density from the semiconductor. Adsorbate binding to the surface occurs when such orbital interactions afford stabilization of occupied orbitals, as seen in Figure 2a,b. Through such mechanisms, the surface charge density and distribution can be altered, enabling analyte detection. Such changes in surface charge may shift the position of E_{fs} and alter the magnitude of ϕ_s.

A measure of the strength of these surface interactions is given by the fraction of adsorbates that are present at the surface in ionized form, representing complete charge transfer and therefore strong binding.[10] For donors, ionization to D^+ corresponds to the generation of a vacant bonding orbital of the surface−adsorbate complex (p-type case in Figure 2a); for acceptors, these orbitals are filled and the adsorbate is then present as A^- (Figure 2b). The newly formed surface−adsorbate molecular orbitals are localized at the surface, and they can therefore be treated as surface states with their electronic occupation given by Fermi−Dirac statistics (eqs 1a and 1b). Rewriting eqs 1a and 1b in terms of the probability of finding the adsorbate in the ionized form gives

$$f(D^+) = [D^+]/[D]_{tot} = 1/[1 + g_{SD}\exp((E_f - E_{SD})/k_bT)] \quad (3a)$$

$$f(A^-) = [A^-]/[A]_{tot} = 1/[1 + g_{SA}\exp((E_{SA} - E_f)/k_bT)] \quad (3b)$$

where E_{SD} and E_{SA} correspond to the energy levels of the donor- and acceptor-stabilized orbitals of the surface−adsorbate complex, respectively (Figure 2); g_{SD} and g_{SA} are the respective degeneracies of these ground states. These functions are shown in the panel on the left-hand side of parts a and b of Figure 2.

According to eqs 3a and 3b, the position of the bulk Fermi level relative to the bonding orbital in the surface complex dictates the fraction of adsorbates that are strongly or irreversibly bound: The fraction

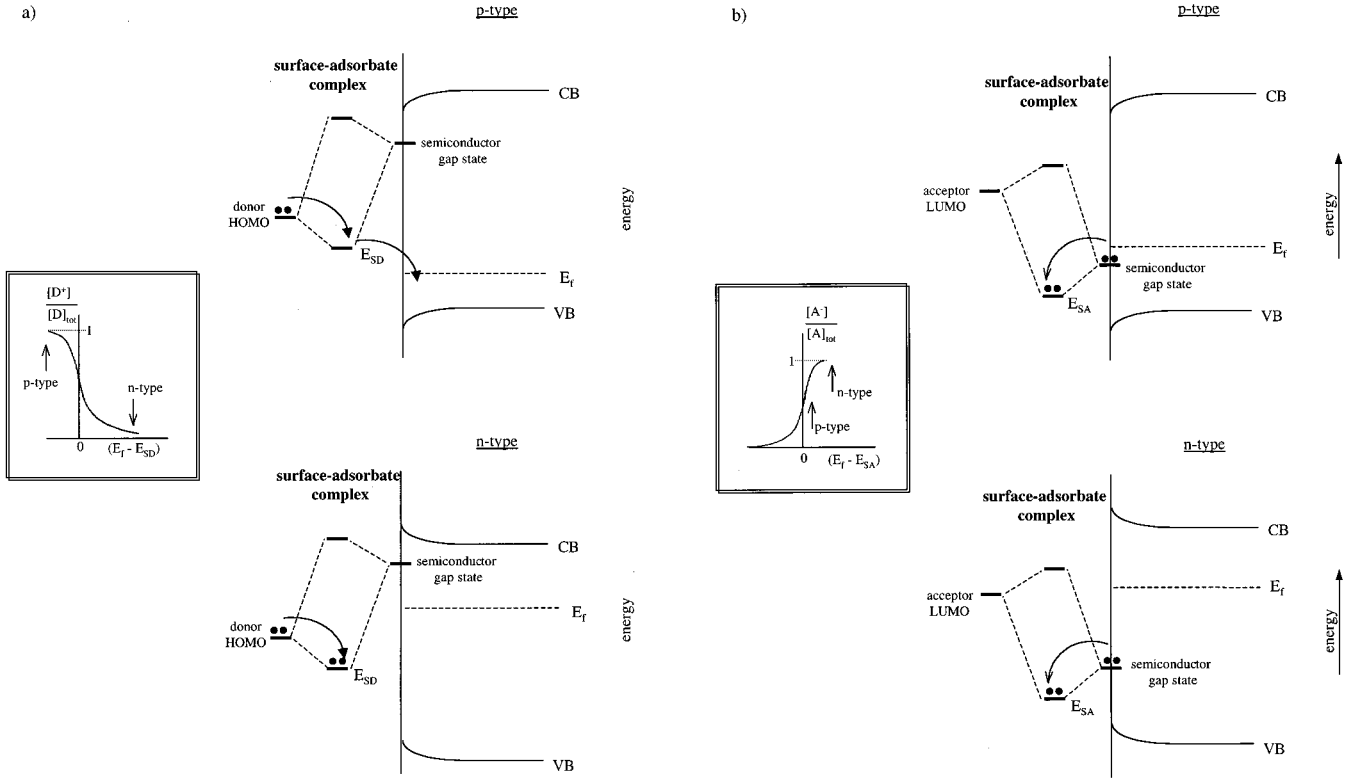

Figure 2. Idealized orbital interactions between surface states and adsorbate molecules. (a) Formation of the surface−adsorbate complex for a donor adsorbate onto a p-type (upper right-hand figure) and n-type (lower right-hand figure) semiconductor substrate. The bonding molecular orbital for the surface−donor complex is indicated by E_{SD}, and the arrows indicate the direction of net transfer of electron density. The left-hand diagram plots the fraction of the donors that are ionized to D^+ as a function of $(E_f - E_{SD})$, with the arrows corresponding to the right-hand illustrations. (b) Formation of the surface−adsorbate complex for an acceptor adsorbate onto a p-type (upper right-hand figure) and n-type (lower right-hand figure) semiconductor substrate. The bonding molecular orbital for the surface−acceptor complex is indicated by E_{SA}, and the arrows indicate the direction of net transfer of electron density. The left-hand diagram plots the fraction of the acceptors that are ionized to A^- as a function of $(E_f - E_{SA})$, with the arrows corresponding to the right-hand illustrations. The conduction band and valence band edges are indicated by CB and VB, respectively. See text for additional explanation.

of strongly bound donors (donors present as D^+) increases as the Fermi level approaches the valence band edge, whereas the fraction of strongly bound acceptors (acceptors present as A^-) increases as the Fermi level approaches the conduction band edge. From the left-hand panel in each of Figures 2a,b, the indicated donor is tightly bound to the semiconductor surface when the substrate is strongly p-type and electron deficient; the acceptor is tightly bound at the surface when the substrate is strongly n-type and electron rich.

For a chemical sensor, this dependence of binding strength on the position of the Fermi level will be reflected in the equilibrium binding constant K and the sensitivity for analyte detection, i.e., the detection limit. Increased sensitivity typically comes with a cost in reversibility, since enhanced charge transfer between adsorbate and semiconductor also implies stronger and more irreversible analyte binding.

It is noteworthy that the energetic distribution and density of surface states can, in some instances, limit the electronic response of a semiconductor toward analytes. For example, bare GaAs has intrinsic surface states with a typical density of $>10^{12}$ cm^{-2} eV^{-1} (except on clean (110) surfaces where there are no surface states in the gap);[20] these states are believed to arise from surface oxide formation.[4−8] Such a high SDOS leads to the presence of a large amount of surface-trapped charge, effectively pinning the surface Fermi level and preventing analyte-induced modulation of band bending. This behavior reflects the fact that even to make a small change in the magnitude of the surface electric field, a relatively large quantity of charge needs to be displaced from the surface states. The result is that the electrooptical properties of such a semiconductor are resistant to external influences such as adsorption, making them unsuitable for chemical detection. As will be discussed below, surface treatments can remove such electronic impediments to chemical sensing in Fermi level-pinned systems.

C. Analyte Binding: Surface States and Carrier Dynamics

Measurements of the electrooptical properties of II−VI and III−V semiconductors that can serve as the basis of chemical sensors will reflect not only the electronic structure of the surface but also the carrier dynamics associated with this structure. Under certain experimental conditions relevant to adsorption, it is possible to identify characteristics associated with the semiconductor surface that dominate its electrooptical properties. Electronic relaxation associated with the solid is commonly described in terms of the surface recombination velocity and

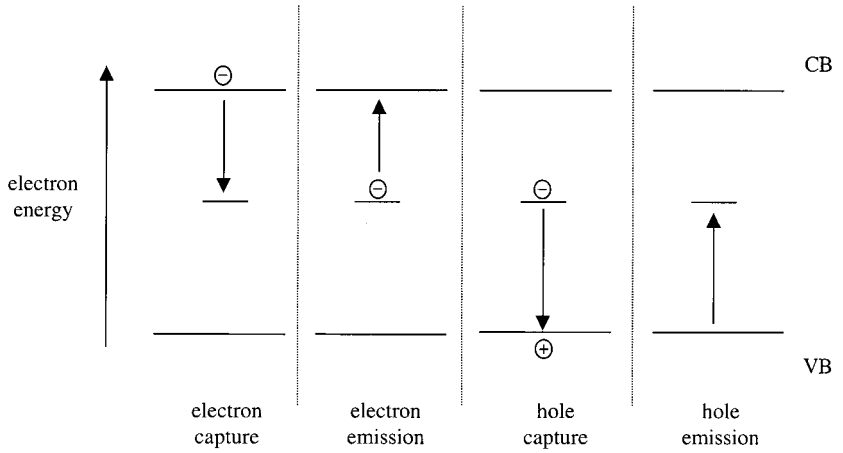

Figure 3. Recombination processes in a semiconductor that are mediated by the indicated mid-gap state. (Adapted from ref 19 with permission from John Wiley & Sons, Inc.)

depletion width. Although the two parameters cannot typically be completely decoupled for the reasons described below, experimental conditions can sometimes be manipulated to highlight one or the other's influence on the interface and susceptibility to adsorption.

a. Surface Recombination Velocity

Recombination processes serve to reestablish the distribution of charge carriers at thermal equilibrium when the semiconductor is perturbed by transient external influences, such as optical or electrical excitation of electrons. Photon and phonon emission resulting from band edge recombination of electron−hole pairs are common relaxation mechanisms. Competing nonradiative recombination processes are mediated through bulk and surface gap states by the processes summarized in Figure 3. The rate at which the system approaches thermal equilibrium through the combined effects of such nonradiative processes is characterized by the recombination velocity. The detailed recombination rate is affected by the entire semiconductor structure and is influenced by the doping, composition, and surface conditions.[19,21] Surface states can exert a substantial influence on the recombination rate because they are typically present at a high density that is difficult to control.

Adsorbed analytes can influence the rate of surface recombination through interactions with surface states, producing an observable change in semiconductor electrical or optical properties under certain conditions. For example, surface states localized near mid-gap are efficient at mediating nonradiative recombination, leading to low PL yields typical of most pinned systems.[19,21] Thus, an adsorbate-induced shift in the energetic position of surface traps away from midgap can produce an increase in semiconductor PL intensity.

Under low injection conditions, recombination is considered a fast event and the rate-limiting step is the generation/transport of minority carriers that must move to the surface. Under such conditions, a relatively small number of excess minority charge carriers are generated as compared to the majority carriers and the expression for the surface recombination velocity, S, can be approximated as[19]

$$S = v_{\mathrm{th}}\sigma N_{\mathrm{ss}} \tag{4}$$

where v_{th} is the thermal velocity of carriers, σ is the carrier capture cross section, and N_{ss} denotes the density of surface states or traps. Adsorbates can modify N_{ss} and σ by introducing or removing surface gap states and by influencing the surface potential, respectively.

Under high injection conditions, recombination at the surface becomes the slow event, since there are more minority carriers generated and transported to the surface than can be easily recombined. This distinction between high and low injection levels is essentially qualitative, with high injection corresponding to situations where the concentration of injected excess carriers is larger or comparable to the concentration of donors or acceptors.

b. Surface Electric Field Effects and the Dead-Layer Model

An electric field near the semiconductor surface sweeps electrons and holes in opposite directions (Figure 1) and can substantially suppress both the majority carrier concentration and electron−hole pair recombination. Modulation of band bending through adsorption of donors and acceptors can affect such semiconductor properties as sample conductance and PL efficiency by influencing recombination properties.

For an n-type semiconductor, adsorbed donors can effectively return surface-trapped charge to the semiconductor bulk, thereby reducing the surface electric field and causing a contraction in the depletion width. Consequently, both the PL intensity and sample conductance can be expected to increase. Similar reasoning for adsorbed acceptors leads to the expectation that the PL intensity and sample conductance should be reduced. As the thickness of the semiconductor approaches the surface depletion width, measurable changes in the conductivity of the sample can be used as a method of analyte detection.

The surface field region is not only an insulating layer, but relatively nonemissive and hence commonly referred to as a "dead layer". Partitioning the semiconductor into a near-surface nonemissive zone of thickness D and an underlying emissive zone is

clearly an oversimplification, but electrical and electrochemical measurements have suggested that the dead-layer model can provide a reasonably good correspondence between the dead-layer thickness, D, and the depletion width, W.[22−24] By influencing the magnitude of the surface electric field, adsorbates can modify the dead-layer thickness. Adsorbate-induced PL behavior is quantitatively related to changes in the thickness of the dead layer according to

$$PL_0/PL_x = \exp(-\alpha'\Delta D) \quad (5)$$

where PL_0 and PL_x are the initial and analyte-induced PL intensities, respectively, α' is the semiconductor absorptivity, corrected for self-absorption ($\alpha' = \alpha + \beta$), and ΔD is the resulting change in dead-layer thickness, $D_0 - D_x$, where D_0 is the initial dead-layer thickness and D_x is the dead-layer thickness in the presence of analyte.[25,26] This model is valid for the special case of a large surface recombination velocity that is not significantly affected by adsorbates (more specifically, $S \gg L/\tau$ and $S \gg \alpha L^2/\tau$, where L and τ are the minority carrier's diffusion length and lifetime, respectively).

A convenient test for the applicability of the dead-layer model is to excite the sample with different interrogating wavelengths, corresponding to a substantial range of penetration depths, and determine whether the PL changes correspond to the same value of ΔD within experimental error. In general, wavelengths whose penetration depths are of approximately the magnitude of the depletion width will provide the most substantial PL responses to analytes, as analyte-induced modulation of the depletion width will yield the greatest fractional changes in the size of the emitting region of the semiconductor.

Probing semiconductor properties under two limiting injection conditions provides further insight into the nature of semiconductor−adsorbate interactions by varying the contributions of surface field effects relative to the recombination processes depicted in Figure 3. At low injection, semiconductor properties can be influenced by the combined effects of adsorbate-induced changes in surface recombination velocity and dead-layer thickness. At high injection, the surface becomes enriched in minority carriers, causing the bands to flatten. This minimizes electric field effects and accentuates the impact of adsorption on surface recombination processes.

Although the conditions above are useful simplifications, complete modeling involves many interdependent processes. For example, for PL, the detailed characterization of the PL response of the semiconductor, and hence the detector response, is affected by many processes that impact the transport and recombination of minority carriers in the near-surface region of a semiconductor.[27,28] These processes are complicated by the presence of nonuniform electric fields in part of the probed volume, which includes the depletion region of the semiconductor. Carrier generation, transport, and recombination processes, together with the spatial distribution, wavelength, and intensity of the probing or exciting radiation, are all factors affecting the quantitative PL response from the semiconductor. The exact state of the semiconductor, and hence the sensor response, under illumination is therefore governed by many factors and is not always amenable to description by analytic expressions. Numerical solution of the coupled partial differential equations governing the recombination and transport of majority and minority carriers in a self-consistent manner with the equations describing the electrostatic fields resulting from these carrier distributions is then required.[27,28]

III. Characterization Techniques for Semiconductor Adsorbates

For irreversibly bound adsorbates, UHV techniques such as PES, vibrational spectroscopy, and diffraction have served admirably to provide information on adsorbate chemical composition and structure. Moreover, in combination with temperature-programmed desorption (TPD), these techniques have provided estimates of the strength of adsorbate binding. For the non-UHV conditions that typically characterize sensor environments, it has been far more difficult to characterize adsorbate chemical composition and structure, particularly for reversibly bound analytes. However, a variety of electrical and optical methods can be used to characterize the effect of adsorbates on a semiconductor's electronic structure in both UHV and non-UHV environments.

Rather than attempting to be exhaustive, the sections below present brief descriptions of the most commonly used characterization tools that serve as the basis for the results highlighted in this review article. References cited in these sections should be consulted for more complete discussions of these techniques and their strengths and limitations.

A. Adsorbate Structure and Composition

a. Photoelectron Spectroscopy (PES)

X-ray photoelectron spectroscopy (XPS) involving core electrons has been invaluable for the compositional analysis of chemically treated semiconductor surfaces.[29,30] Shifts in the core levels of adsorbate and substrate atoms provide information about changes in chemical character. Depth profiling of surface films, commonly achieved by varying the angle of incidence of the X-ray beam, can reveal information on composition as a function of distance from the surface. However, the applicability of conventional XPS techniques is limited owing to the low spectral resolution and relatively poor surface sensitivity associated with the use of standard hard X-ray sources.[31] The availability of synchrotron radiation as a source of intense, tunable soft X-rays (30−350 eV) has revolutionized photoemission techniques, providing spectral resolution to better than 0.4 eV and superior surface sensitivity, with probe depths as shallow as 5−10 Å.

Strongly electronegative adsorbates, such as halogens and oxygen, typically induce substantial shifts (0.5−1.0 eV) of semiconductor atom peaks, making chemical assignments reasonably straightforward.[5,32] However, characterization of many other semicon-

ductor-derived interfaces has demanded the higher resolution and improved surface sensitivity offered by synchrotron facilities. For example, as will be discussed in detail in subsequent sections, the possibility of Fermi level unpinning resulting from sulfide treatment of GaAs surfaces requires identification of surface bonding in order to understand the apparently critical role of adsorbed sulfides. However, sulfur-induced chemical shifts of GaAs-based peaks are subtle (less than 0.5 eV), accounting for much of the controversy involving surface site-selectivity in the early literature that relied on conventional XPS characterization. Direct analysis of adsorbed sulfur has also been challenging by conventional XPS, owing to its very small photoionization cross-section and a shallow escape depth (2 nm) characteristic of sulfur photoelectrons.[33]

b. Surface Vibrational Spectroscopies

Both high-resolution electron energy loss spectroscopy (HREELS) and attenuated total reflection (ATR) IR spectroscopy are powerful techniques for characterizing the surface bonding and orientation of adsorbates.[34−38] HREELS is a UHV technique involving inelastic surface scattering of incident low-energy electrons. As a result of the scattering event, surface-bound species become vibrationally excited and electron energy losses at specific energies corresponding to vibrational modes of the adsorbate are observed. Attractive features of HREELS are its superior sensitivity and ability to access the spectral region below 400 cm^{-1}, which is usually not amenable to standard IR techniques. However, the spectral resolution of HREELS is typically only 40−80 cm^{-1}, although recent instrumental advances have improved resolution to better than 10 cm^{-1}.[39] An additional advantage of reflection IR techniques is that an UHV environment is not required, making it better suited for studying weakly adsorbed species.

c. Diffraction Techniques

Diffraction techniques provide important structural information, provided the adsorbed layer has long-range order.[39] Surface-sensitive electron diffraction techniques, such as LEEDS (low-energy electron diffraction spectroscopy) and RHEEDS (reflection high-energy electron diffraction spectroscopy), are routinely used to monitor the structure of an adsorbed film as a function of chemical and annealing treatments and for initial characterization of the surface reconstruction of the bare semiconductor surface. However, these methods do not provide microscopic structural details about bonding to the surface. Chemical state-specific photoelectron diffraction (PED) is a powerful technique that combines the chemical specificity of photoelectron techniques with the structure-solving capability of diffraction techniques and has been used in determining the surface structure of chemisorbed species. This method allows the determination of the surface structure owing to a particular chemical species by selectively monitoring the diffraction pattern generated by electrons emitted from the atoms of interest.[40,41]

d. Other Techniques

In addition to the aforementioned techniques, reflectance anisotropy spectroscopy (RAS) has recently been developed to probe the presence of oriented surface dimer species on polar semiconductors.[42−45] This technique relies on the low symmetry of the surfaces of cubic semiconductors and is based on measuring the difference in reflectivity of polarized light along two orthogonal axes of the surface. The bulk contribution disappears in this analysis, making the measurement sensitive to the presence of surface adsorbates aligned with the two axes, even when the adsorbates are covered by an amorphous overlayer. However, the interpretation of the RAS spectral signal is often difficult. The technique has been used successfully to observe the appearance and removal of surface dimers of Ga or As on GaAs surfaces.[44,45]

Temperature-programmed desorption (TPD) provides a surface compositional analysis based on mass spectrometry of desorbed adsorbates. The sensitivity of mass spectrometric detection allows analysis of coverages less than 0.1% of a monolayer.[46] The desorption temperature indicates the strength of surface binding and has been used to infer the presence of different binding sites at the surface, as well as to distinguish between chemisorbed and physisorbed species. For example, using TPD, along with supporting information from HREELS analysis, Chung and Yi et al. provide evidence for the presence of molecularly adsorbed and dissociatively adsorbed H_2S on the Ga-rich GaAs (100)−(4 × 2) surface.[47,48]

Scanning probe microscopies (SPM), such as scanning tunneling microscopy (STM) and atomic force microscopy (AFM), are extremely useful techniques, providing direct observation of local surface structure at the atomic scale (∼1 Å) and characterization of surface morphology at larger length scales (∼25 Å).[49] Local structural information complements the average surface structure provided by other techniques and can be critical for understanding local adsorption phenomena. However, SPM studies of adsorbate structure on semiconductor surfaces is often challenging, and few such studies are currently available. Some examples are discussed in section IV.C.

B. Adsorbate Effects on Semiconductor Electronic Properties

a. Electrical Methods

Electrical properties such as sample conductance, capacitance, and work function can provide adsorption signatures for chemical detection as well as allow estimation of analyte effects on such quantities as E_{fs} and the surface densities of states (SDOS). These methods require an electrical contact to be made to the sample. The contacts do not have to be over the surface region of interest but merely electrically connect the surface region to an outside contact. In fact, care must be taken in order to prevent changes in the structure or chemistry of the surface region targeted for investigation due to the process of contact formation. Often, subsequent surface prepa-

ration and treatment of the region of interest can be carried out after contact formation.

Once contacts are established, electrical measurements can provide estimates of surface charge, from which SDOS are often inferred. Electrical properties are commonly measured using Schottky diodes or metal−insulator−semiconductor (MIS) devices incorporating the surface-modified semiconductor sample as an active component. A semiconductor adsorbate then becomes part of a buried interface. In this case, of course, the properties of the adsorbate-modified interface may be perturbed by the coating.[50−52] Measurements of capacitance and current of these devices as a function of applied voltage (C−V and I−V curves, respectively) provide information about the flatband potential and donor density.[19,53,54] The device response to high- and low-frequency modulation of the applied voltage reflects the kinetic trapping characteristics of the surface states.

The Kelvin probe or contact potential difference (CPD) method is a means by which the work function difference between two surfaces can be determined. This is a nondestructive technique based on the measurement of capacitance between two surfaces separated by a small gap. With the surfaces in electrical contact through an external circuit, the difference in work function between the two materials results in a potential difference, the contact potential. The separated surfaces form a capacitor with a charge resulting from the work function difference. As the separation between the plates oscillates at a known frequency, the observed time-varying capacitance can be related to the contact potential.[55,56] In the case of semiconductor surfaces, the difference in work function can be related to the Fermi level position within the material. The work function can be modified not only by the presence of analytes, but also by surface contamination, making the determination of the specific work function within the material challenging but potentially useful for estimating adsorbate effects on ϕ_w.

b. Optical Methods

Optical methods do not require any electrical contact with the sample and generally are nondestructive. In this regard, they can have an advantage over electrical measurements. The methods most commonly used include PES, Raman spectroscopy, photoreflectance (PR), and steady-state and time-resolved photoluminescence (PL) measurements.

PES, Raman, and PR provide information about the position of the surface Fermi level, E_{fs}. The data generally need to be corrected for a surface photovoltage induced by the measurement. Surface Fermi level shifts are obtained from global shifts in the core-level PES spectra as measured relative to a reference. However, Berkovits et al. recently demonstrated that when intense X-rays are used in PES, photocleavage of surface-bound species can occur.[57] Raman spectroscopy also requires the use of an intense excitation source, which can lead to unwanted surface photochemistry; furthermore, this technique also suffers from low signal-to-noise ratios.[58] Photoreflectance is a well-established technique for measuring the surface electric field in semiconductors and has recently been used to estimate the surface state density of an H_2S plasma-treated GaAs surface.[59,60]

Optical methods for measuring properties directly related to surface states, such as their energetic location and density, are relatively few in number. Besides PR, other probes of surface states that have been used include thermally stimulated exoelectron emission (TSEE) and a surface state spectroscopy method based on PL developed by Saitoh et al.[61,62] By probing filled defect states near the surface, PR and TSEE techniques provide the energetic position of these defects relative to the band edges. Saitoh et al. used their PL-based surface state spectroscopy method to estimate the SDOS. By modeling the PL yield as a function of ultra-band gap excitation intensity, they have inferred the shape and density of the surface state distribution.

Comparison of PL at high and low injection limits has provided further information on the effects of adsorbates on the semiconductor's electronic structure. As noted earlier in section II.C, nearly flattened bands, corresponding to high injection conditions, have been used to decouple surface electric field effects from surface recombination velocity effects. Adsorbate-induced changes in steady-state PL intensity under low injection conditions can indicate modified surface properties. Ellis et al. used such variations in steady-state PL intensity to obtain quantitative estimates of changes in the thickness of the dead-layer region resulting from adsorption.[1] Time-resolved PL measurements complement such measurements and have been used to estimate surface recombination velocities.[63−67]

IV. Surface Modification

The development of a chemical sensor technology based on II−VI and III−V semiconductors is dependent on the ability to prepare stable semiconductor surfaces with tailored surface properties. Initial preparation of surfaces usually involves etching in order to obtain a fresh surface, and section IV.A reviews commonly used chemical etching techniques for prototypical II−VI and III−V semiconductors. More sophisticated surface modification strategies involve subsequent coating of the surface with transducer films (section IV.B) and the use of passivation methods to prepare tailored surfaces (section IV.C).

Obtaining stable surface properties is usually the first step toward the goal of tailored surfaces. This step is also the greatest challenge, as most semiconductor properties degrade over time, especially with exposure to oxygen and moisture. For this reason, many studies of semiconductor surfaces are usually performed under pristine conditions (typically UHV after ion bombardment and subsequent annealing) in order to study molecular interactions with a reproducibly clean surface. However, reproducible adsorbate-induced effects have also been reported with II−VI and III−V surfaces handled under far less stringent conditions, typical of most sensor applications. These surfaces had been modified with particular surface treatments based on chemical etching, transducer films, and passivation methods. Because

the development of controlled surface modification strategies is a critical precursor to chemical sensor applications of II−VI and III−V materials, the following sections provide a summary of the current knowledge in these areas.

A. Wet Chemical Etchants

Etchants promote vigorous chemical reactions with semiconductors that can influence surface chemical composition as well as dictate the surface morphology. Systematic studies of the effects of reaction conditions on semiconductor surface composition and morphology are rare. It has become apparent, though, that the structure and composition of a surface resulting from an etching treatment is generally a complex function of temperature, etchant composition and concentration, etch duration, diffusivity of reagents in solution, and initial semiconductor surface composition and structure.

An extensive summary of etchants for III−V and II−VI materials has been published,[68] and another review addresses issues specific to GaAs and GaP along with group IV semiconductors.[69] Stirland and Straughan reviewed the etching literature specifically for GaAs in 1976.[70] Much of the current information about etchants is still largely empirical. In general, this is an area that is ripe for more comprehensive and detailed mechanistic work, particularly with the improvements in analytical instrumentation that have occurred.

As might be expected from the relative chemical stability of II−VI and III−V compounds, strong oxidants are typically needed to effect etching. Solution conditions are commonly adjusted to obtain soluble products in reasonable periods of time. Two of the most widely used and studied etchants are bromine in methanol and alkaline peroxide. Their effects on prototypical compound semiconductors, described below, illustrate many of the issues associated with wet chemical etching of relevance to adsorption experiments and the kind of information that is currently available.

a. Bromine in Alcohol

Treatment of surfaces of II−VI (CdS, CdSe, CdTe) and III−V (GaAs) semiconductors with alcoholic solutions of bromine is a common method for preparing fresh surfaces. With the development of alternate etchants better suited for GaAs, the use of bromine treatments is generally found with II−VI materials.

The bromine-induced etching behaviors of polycrystalline CdTe and single-crystal GaAs have been compared in a novel study by McGhee and coworkers, using radiolabeled bromine vapor, ^{82}BrBr, to track the progress of the etching reactions.[71] These two materials were found to differ significantly in etching behavior: The overall radioactivity of the GaAs sample was found to continually increase with exposure to ^{82}BrBr, whereas that of CdTe reached a saturation value, upon which further exposure to ^{82}BrBr had no effect on the radioactivity. The authors propose that volatile products, such as $AsBr_3$, are formed in the reaction with GaAs, whereas a nonvolatile coating results on the CdTe surface, which prevents further reaction with bromine. This difference persisted for etching in the presence of a solvent, with the only apparent effect of the solvent being to reduce the etching reaction rate. The uncontrolled nature of bromine etching of GaAs results in rough surfaces, and for this reason, the treatment is usually not favored for the preparation of GaAs surfaces.

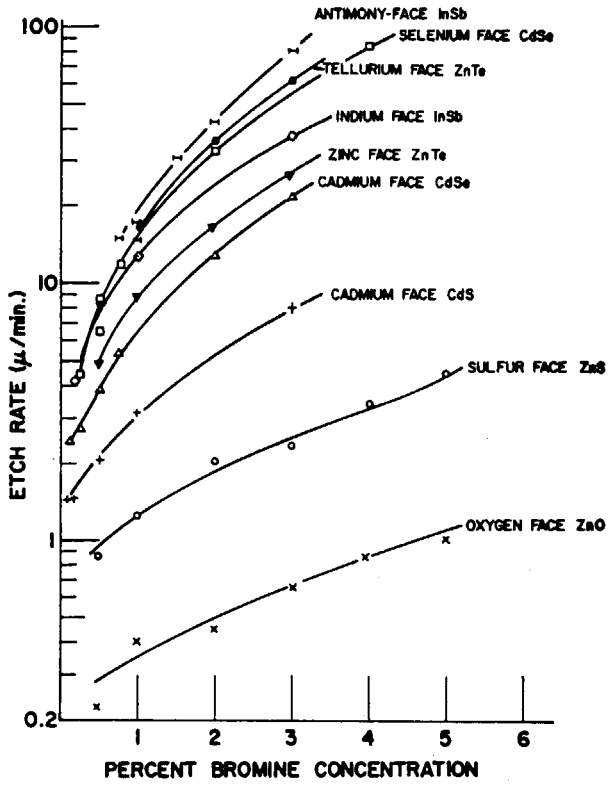

Figure 4. Etch rate at room temperature for the anion faces of ZnO, ZnS, CdSe, ZnTe, and InSb and for the cation faces of CdS, CdSe, ZnTe, and InSb, versus bromine concentration in methanol. (Reprinted from ref 72.)

In early studies of II−VI semiconductors, Strehlow found a correlation between reactivity toward bromine/methanol etchant and the difference in electronegativity between the two components of the material: Faster etch rates were obtained with smaller differences in electronegativity between the two elements comprising the II−VI semiconductor.[72] This correlation is shown in Figure 4. Since then, Komisarchik and co-workers conducted the most complete set of studies of alcoholic bromine etches of CdSe and CdTe surfaces.[73−75] These researchers report that the age of the etching solution appears to play an important role in determining the final surface composition of the Se-rich $(000\bar{1})$ surface. For example, fresh Br_2/ethanol solutions were reported to produce a near-stoichiometric surface, slightly depleted in cadmium, as evidenced by a Cd:Se ratio of 0.91 from X-ray photoelectron spectroscopy studies (XPS). In contrast, aged solutions (∼5 h) resulted in a Cd-rich surface (Cd:Se ≈ 1.6 by XPS). Hydrobromic acid, which is known to accumulate in this etching solution over time, may be partly responsible for the observed differences in surface composition.[74,76]

Selective etching is also found for the (110) surface of p-CdTe resulting from Br_2/methanol treatment.

According to XPS results, the surface is depleted in cadmium, as evidenced by a Cd:Te ratio of ~0.7.[77]

Selective removal of surface atoms by the etchant suggests that the efficacy of an etch should depend on the crystal face being exposed. Unfortunately, few studies have involved a direct comparison of different crystal faces and available results appear to be in disagreement. For example, according to electrochemical measurements by Hodes et al., there is no preferential etching among the (0001), (10$\bar{1}$0), and (11$\bar{2}$0) crystal faces of CdSe for Br_2/methanol and aqua regia etches.[78] In contrast, Hickman et al. identified preferential etching of different faces on the basis of SEM results.[79] Komisarchik and co-workers found that the (0001) and (000$\bar{1}$) faces of CdSe are indistinguishable based on their similar etch rates.[73] The inability to distinguish the rates of reaction for these two faces of CdSe contradicts earlier work by Strehlow, who reported that the anion-rich faces typically exhibit accelerated etch rates relative to the cation-rich faces for a variety of II−VI compounds. This difference has been attributed to the electrophilic nature of the etchants and enhanced accessibility to chalcogen atoms on anion-rich faces.[72]

Bromine contamination of the surface resulting from the Br_2/alcohol etching treatment has been reported as being slight, an attractive feature of this particular treatment.[74] Reaction products that may be deposited at the surface include $CdBr_2$, elemental chalcogen, and various chalcogenide bromides, including A_2Br_2 and ABr_4, for A = Se, Te.[73,75,77]

Studies suggest that the surface morphology is a strong function of bromine concentration. Investigations of the CdTe(110) surface indicate that at low bromine concentrations, a relatively smooth surface is produced, whereas a rough and pitted surface remains when high bromine concentrations are used.[80]

Following etching treatments, surface oxide formation rapidly occurs upon exposure to air. From ellipsometry measurements of CdSe, the oxide layer has been found to be about 3 times thicker on the Se-rich (000$\bar{1}$) face as compared to the Cd-rich (0001) face, suggesting that the Se-rich face is more susceptible to oxygen attack.[74] This result is consistent with the appearance of a dull side and a shiny side following etching with bromine/methanol. Interestingly, Komisarchik and co-workers also noted that the thickness of the oxide layer on the Se-rich (000$\bar{1}$) face was correlated with duration of etching, with a thicker oxide resulting when a prolonged (>5 min) etch had been used. In contrast, the oxide thickness on the Cd-rich (0001) face showed no such dependence. Preferred oxidation of the Se-rich face has also been noted by Bowen Katari et al. for CdSe nanocrystals, which feature a number of different exposed crystal faces.[81] It should be noted that a preference for cadmium oxidation has been reported for the (11$\bar{2}$0) cleaved, nonpolar CdSe surface by Brillson in his study conducted in a controlled UHV environment.[82]

b. Peroxide

Alkaline peroxide etches are commonly used for preparing fresh GaAs surfaces, with the alkaline component typically being sodium hydroxide or ammonia. Surface oxides and hydroxides are usually present, and the surface composition is sensitive to the pH of the etch solution. For example, for alkaline solutions of pH < 10, hydrogen peroxide exposure leads primarily to surface oxide and hydroxide formation, specifically Ga_2O_3 and $Ga(OH)_3$, through such reactions as[83]

$$-Ga-As- \xrightarrow{H_2O_2} HO-GaAs-OH \xrightarrow{2H_2O_2} Ga(OH)_3/As(OH)_3 \quad (6)$$

Increasing the pH from 10 up to about 12, using sodium hydroxide, results in the removal of surface hydroxides through solubilization of these species according to

$$Ga(OH)_3 + 3OH^- \rightarrow GaO_3^{3-} + 3H_2O,\ 10 < pH < 12 \quad (7)$$

Kelly and Reynders noted that the optimum pH range for peroxide etching is 10−12, because at pH < 10 formation of a surface oxide film prevents effective etching whereas for pH > 12 peroxide is highly dissociated ($pK_a = 11.6$), leading to slow etch rates.[83]

To reduce surface oxygen contamination, complexing agents such as ammonia and EDTA can be used instead of sodium hydroxide. Such additives can coordinate to surface gallium atoms to form soluble gallium species, such as $Ga(NH_3)_m^{3+}$ when ammonia is used, thereby etching the GaAs surface.[83] Bryce and Berk also attributed the etching effect of ammonia to solubilization of surface As_2O_3 to form $(NH_4)_3AsO_4$.[84]

Kelly et al. compared the rates of the ammonia/peroxide etch for different crystal orientations of GaAs.[83] The relative etching rates were found to follow the order As-rich (111) face ≈ (100) face > Ga-rich (111) face, with the relative rates spanning about a factor of 4.

Acidic peroxide etches are also used but usually result in the formation of a substantial amount of surface arsenic-bound oxygen, as found in XPS studies by Massies and Contour.[85] Acids used include sulfuric, phosphoric, citric, nitric, and hydrochloric.[85−87]

B. Transducer Films

Coating semiconductor substrates with films represents a versatile methodology for surface modification that provides new opportunities for chemical sensing. Various coating procedures have been employed, ranging from deposition of metal and polymer films, to growth of surface coordination polymers derived from the semiconductor surface, to dip-coating. Once created on the semiconductor substrate, the chemistry of the film has the ability to influence the electrooptical properties of the II−VI or III−V substrate, thereby modifying and/or providing a transduction mechanism for chemical sensing.

Early experiments directed toward chemical sensing involved deposition of Pd films onto CdS substrates.[88,89] Exposure to hydrogen gas caused a substantial PL enhancement and change in current−voltage properties, which were attributed to a lowering of the work function of the metal through formation of Pd hydride phases; the PL effect was reversible upon returning to a nitrogen ambient. Coating Pd onto a graded CdS_xSe_{1-x} substrate, which produces PL spanning the band gaps of the compositions comprising the graded region, altered the PL spectral distribution, with greater enhancements corresponding to PL from compositions closer to the surface.[89]

An example of chemical sensing based on net redox chemistry was reported for a GaAs substrate coated with a polymer prepared from (1,1′-ferrocenediyl)-dichlorosilane.[90] Exposure to volatile oxidants such as iodine or bromine quenched the GaAs PL intensity in accord with the dead-layer model (section II.C). The effect could be reversed by exposing the film to the vapor of the strong reductant hydrazine. This system effectively functions as a dosimeter, since a reagent is needed to restore the film to its original state.

Examples of II−VI semiconductor-derived coordination polymer films have been reported by Bocarsly et al. and Licht et al. as having superior photoelectrochemical stability. They used CdS(e) samples as photoanodes in solutions containing metallocyanide complexes such as $Fe(CN)_6^{4-}$ to grow coordination polymers. Because these films can exchange countercations, affecting the microstructure and semiconductor-film interfacial charge-transfer properties, they may have potential for chemical sensing applications.[91,92]

Transducer films for gaseous analytes have been studied by Ellis et al. using CdSe substrates. Noting that a variety of gaseous molecules such as oxygen, carbon monoxide, and carbon dioxide do not elicit a PL response from CdSe relative to a reference ambient like vacuum or nitrogen, they explored whether coatings comprising molecules that react reversibly with such species could cause a PL response in the underlying semiconductor. In a number of cases reversible PL responses could be observed, thereby expanding the range of analytes embraced by this methodology. A summary of the films used and analytes detected with them is presented in Table 1.

The PL responses obtained also permit characterization of the buried semiconductor−film interface when binding constants estimated from concentration-dependent PL changes are compared with those acquired from techniques such as IR and UV−vis spectroscopy.[93] The basis for this novel interfacial characterization method is that techniques such as IR and UV−vis spectroscopy typically sample the entire bulk film, whereas the PL technique is sensitive generally to the few monolayers of the film that lie closest to the semiconductor surface. The equations involved are shown below for the binding of an analyte A to bulk film, **1**(f), or to the film molecules occupying semiconductor surface sites, **1**·σ:

$$\mathbf{1}(\mathrm{f}) + \mathrm{A} \Leftrightarrow \mathbf{1}\cdot\mathrm{A}(\mathrm{f}) \quad \text{monitored by IR/UV−vis} \tag{8}$$

$$\mathbf{1}\cdot\mathrm{A}(\mathrm{f}) + \mathbf{1}\cdot\sigma \Leftrightarrow \mathbf{1}\cdot\mathrm{A} \bullet \sigma + \mathbf{1}(\mathrm{f}) \quad \text{distribution or partition coefficient} \tag{9}$$

$$\mathbf{1}\cdot\sigma + \mathrm{A} \Leftrightarrow \mathbf{1}\cdot\mathrm{A}\cdot\sigma \quad \text{monitored by PL} \tag{10}$$

Since the first two equilibria sum to the third, the ratio of equilibrium constants obtained from IR/UV−vis (first equilibrium) and PL (third equilibrium) can yield an estimate of the partition or distribution equilibrium that characterizes the preference for the analyte to bind in the bulk film vs at the semiconductor surface.

For some films, the analyte appears to have no preference between bulk film and semiconductor−film interface environments. For example, deposition from methylene chloride of *N,N′*-ethylenebis(3-methoxysalicylideneiminato)cobalt(II) [Co(3-methoxysalen)], which is known to bind oxygen reversibly in the solid state by forming an O_2-bridged dimer, yields a reversible CdSe PL response to oxygen.[94] The binding constant of oxygen in the film agreed with the value previously reported from X-ray diffraction measurements by Calvin et al., suggesting a partition coefficient near unity.[95] Likewise, deposition of the bifunctional alkanolamines ethanolamine, 3-aminopropanol, and 4-aminobutanol on CdSe, which permitted reversible detection of carbon dioxide via carbamate formation, yielded similar concentration-dependent binding profiles by PL and by IR.[96]

Deposition of Vaska's complex, *trans*-ClIr(CO)-$(PPh_3)_2$, onto CdSe allowed detection of both carbon monoxide and oxygen, with the former causing an enhancement and the latter a quenching of PL intensity from the substrate. However, whereas the concentration profiles for carbon monoxide binding by IR and PL were experimentally indistinguishable, the oxygen binding profiles determined by IR and PL differed substantially, corresponding to roughly an order of magnitude preference for binding oxygen at the semiconductor−film interface, Figure 5. The enhanced affinity was attributed to the potential for chelation by the complex at the CdSe surface, as sketched in Figure 6.[93]

The potential scope of this strategy for imparting selectivity to binding is illustrated by the demonstrations that both chiral films and metalloporphyrins can be employed for analyte detection. For example, films of Jacobsen's catalyst on CdSe have proven capable of discriminating among the four stereoisomers of phenylpropylene oxide through gas-phase PL responses.[97] Metalloporphyrin films derived from divalent metals and octaethylporphyrin (OEP) and tetraphenylporphyrin (TPP) ligands have been used to detect oxygen.[98,99] Nitric oxide has recently been detected using trivalent FeTPPCl and CoTPPCl films.[100] Comparisons of PL with IR/UV−vis spectral changes reveal that NO has a strong aversion to binding at the semiconductor−film interface, as opposed to the bulk film environment.

Table 1. Response of CdSe PL to Representative Analytes[a]

film/analyte[b]	PL response direction	log K[c]	ref
Co(3-MeO-salen)/O_2	quench	2−3	94
Vaska's complex/O_2	quench	3	93
Vaska's complex/CO	enhancement	2	93
Jacobsen's catalyst/ phenylpropylene oxide	enhancement	4−5	97
ZnOEP/O_2	quench	1−2	98
NiTPP/O_2	enhancement	1−2	98
CoTPPCl/NO	enhancement	1	100
Group III Analyte[d]			
$MeBBr_2$ (g)	quench	4	194
Et_3B (g)	quench	3	194
Me_3Ga:NMe_3 (g)	enhancement	5	195
Group IV Analyte[d]			
1,3-butadiene (g)	enhancement	2	196
TCNQ/CH_2Cl_2	quench	5−6	192
C_{60}/toluene	quench	5−6	193
C_{70}/toluene	quench	5−6	193
Me_2EtSiH (g)	enhancement	4	198
Me(n-Pr)SiH_2 (g)	enhancement	3	198
Group V Analyte[d]			
NH_3 (g)	enhancement	3−4	186,199
$MeNH_2$ (g)	enhancement	3−4	186
PH_3 (g)	enhancement	4	199
AsH_3 (g)	enhancement	4	199
Aniline/toluene	enhancement	3	200
$NH_2CH_2CH_2NH_2$/ cyclohexane	enhancement	4	190
$CH_3CH_2CH_2NH_2$/cyclohexane	enhancement	2	190
o-phenylenediamine/ cyclohexane	enhancement	4	190
o-toluidine/ cyclohexane	enhancement	2	190
PPh_3/toluene	enhancement	1	202
$PEtPh_2$/toluene	enhancement	2	202
Group VI Analyte[d]			
acetaldehyde/ cyclohexane	quench	2	191
acetophenone/ cyclohexane	quench	3	191
benzophenone/ cyclohexane	quench	3	191
benzaldehyde/ cyclohexane	quench	3	191
benzil/cyclohexane	quench	4−5	191
2,3-butanedione/ cyclohexane	quench	4−5	191
2,4-pentanedione/ cyclohexane	quench	2	191
1,4-benzoquinone/ cyclohexane	quench	4−5	191
phenanthrenequinone/cyclohexane	quench	5−6	191
tri-*n*-octylphosphine oxide/toluene[e]	enhancement	4	209
Me_2S (g)	enhancement	2−3	210
Me_2Se (g)	enhancement	2−3	210
Et_2S (g)	enhancement	3−4	210
$(t\text{-}Bu)_2S$ (g)	enhancement	4	210
Metal Complex Analyte[d]			
$Pr(fod)_3$/isooctane	quench	2−3	212
$Gd(fod)_3$/isooctane	quench	3	212
$Yb(fod)_3$/isooctane	quench	3	212
Co(3-MeO-salen)/CH_2Cl_2[e]	enhancement	4−5	94
Vaska's complex/toluene/N_2[f]	enhancement	4−5	93
Vaska's complex/toluene/CO[f]	enhancement	4−5	93
Vaska's complex/toluene/O_2[f]	quench	6−7	93
TPP/CH_2Cl_2	enhancement	3−4	98
OEP/CH_2Cl_2	enhancement	3−4	98
MgTPP/CH_2Cl_2/N_2[f]	quench	3	98
MgTPP/CH_2Cl_2/O_2[f]	enhancement	3	98
NiTPP/CH_2Cl_2/N_2[f]	quench	3−4	98
NiTPP/CH_2Cl_2/O_2[f]	enhancement	3−4	98
NiOEP/CH_2Cl_2/N_2[f]	quench	5	98
NiOEP/CH_2Cl_2/O_2[f]	enhancement	5	98
CoTPP/CH_2Cl_2/N_2[f]	enhancement	4−5	98
CoTPP/CH_2Cl_2/O_2[f]	enhancement	3−4	98
CoTPPCl/N_2	quench	4	100
CoTPPCl/NO	enhancement	4	100
Bifunctional Analyte[d]			
$NH_2CH_2CH_2OH$/THF	enhancement	1−2	96
$NH_2CH_2CH_2CH_2OH$/ THF	enhancement	2−3	96
p-phenylenediamine/THF	enhancement	4	96
trans-1,4-diamino-cyclohexane/THF	enhancement	1−2	96

[a] Effects on PL intensity relative to a reference ambient (the indicated solvent or, for gaseous analytes, vacuum or nitrogen) for single-crystal CdSe samples whose (0001) face is irradiated. [b] Response of the coated CdSe surface to the indicated analyte. [c] Logarithm of the adsorption binding constant, $K(M^{-1})$, obtained from PL changes using the Langmuir adsorption isotherm model (eq 12). [d] Response of the bare CdSe surface to the indicated analyte. [e] At low concentrations; at high concentrations, irreversible PL changes occur. [f] The solution is saturated with the indicated gas.

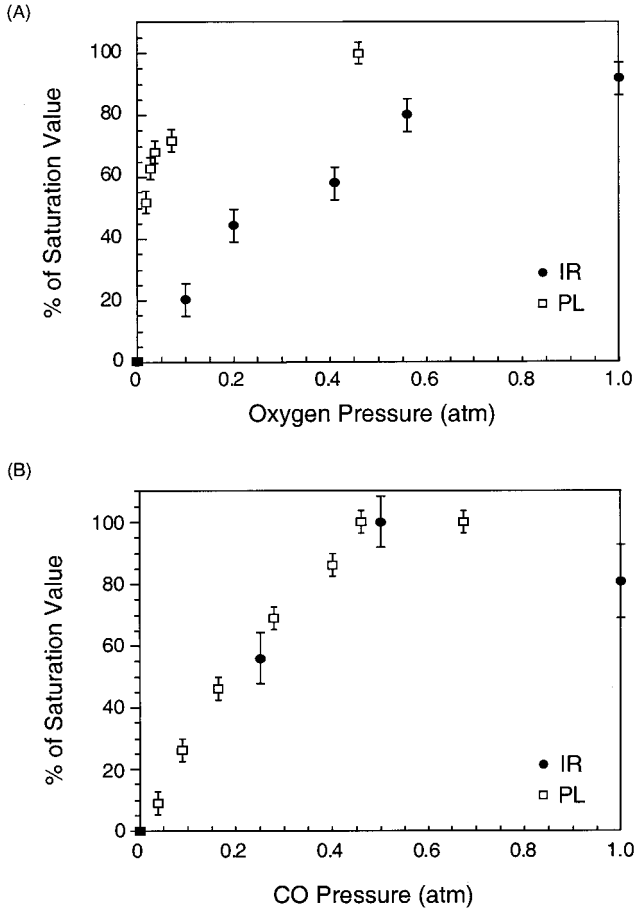

Figure 5. Normalized IR responses of a film of Vaska's complex on a NaCl plate and of PL responses (change in dead-layer thickness) of a film of the complex on CdSe to changes in (A) oxygen and (B) carbon monoxide partial pressure. Saturated spectroscopic changes were set to 100%, and intermediate values are expressed as percentages of the saturation values. (Reprinted from ref 93.)

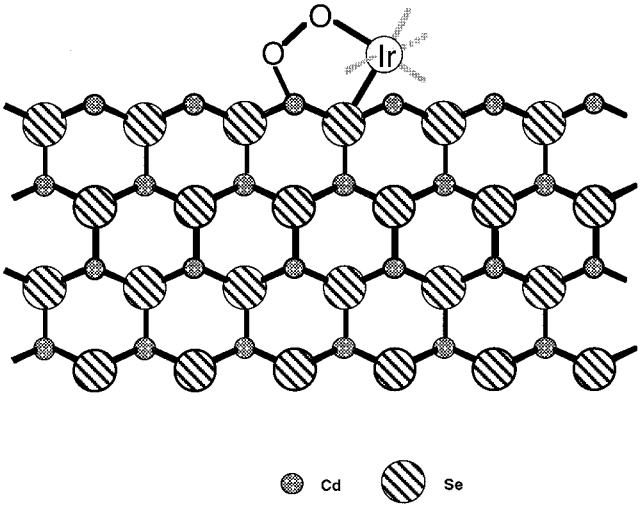

Figure 6. Possible chelating binding mode of the oxygen adduct of Vaska's complex at the CdSe surface. (Reprinted from ref 93.)

A noteworthy aspect of film-coated semiconductors is that in some instances film chemistry may be exploited to tune sensor characteristics. For the Co(3-methoxy-salen) complex described above, the magnitude and speed of the film response depends on the excitation wavelength and intensity, as the film appears to release oxygen upon direct photoexcitation. This suggests a strategy of using photoexcitation at a wavelength not absorbed by the film to monitor the presence of an analyte and then to hasten desorption of the analyte from the film by exciting at a wavelength absorbed by the film. More generally, the analytes present in a film and their concentration might be manipulated by judicious choice of excitation conditions.

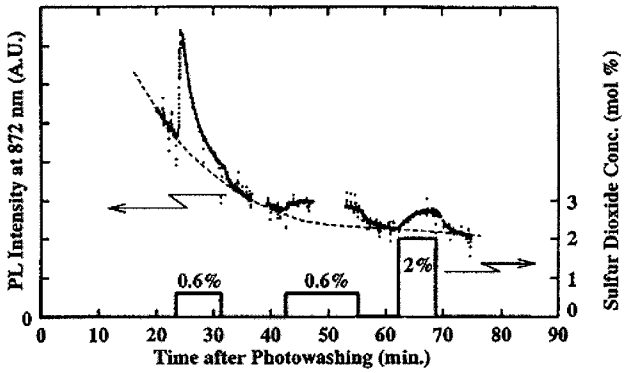

Figure 7. PL intensity at 872 nm (left-hand scale) from a sample with a 2-μm-thick n-GaAs surface layer (carrier concentration of 3×10^{16} cm^{-3}) as a function of time after a photowashing procedure and intermittent exposure to SO_2 (in nitrogen carrier gas); the SO_2 concentration is plotted using the right-hand scale. The dashed line shows the assumed baseline PL (with no SO_2). (Reprinted from ref 28.)

C. Passivation Methods and Tailored Surfaces

Owing to the ever-growing importance of GaAs and related III−V semiconductors in electronic devices, there has been considerable effort directed toward finding methods that yield stable, electronically passivated surfaces. The term "passivation" has several uses in the semiconductor literature.[4,101] One use of the term is for a surface treatment that does not necessarily have an effect on electronic structure but prevents other contaminants from binding to the surface (oxide formation, e.g., as a mechanism for inhibiting adsorption of carbon). In other contexts the term describes modification of electronic states. We will use the term here to refer to treating a surface chemically so as to alter the surface state density and unpin the Fermi level. This kind of passivation can be accomplished in a variety of ways and for varying periods of time through gas-phase chemical and physical treatments and by solution treatments.

An early report of temporary surface passivation involved immersion of illuminated GaAs in flowing water.[102−104] Hirota et al. report RHEED studies of (001) GaAs surfaces prepared with RDIW (running deionized water) treatments.[103] They found that an arsenic-rich surface is frequently the product after RDIW treatment. An illustration of a short-lived SO_2-induced PL response following such a passivation treatment is shown in Figure 7.[28]

Sustained passivation effects have been achieved through sulfide and halogen surface treatments, which are described in sections below. These studies underscored the importance of specific binding in-

teractions of the Ga and As atoms and have led to a variety of strategies for achieving site-selective surface chemistry. Such control of the surface at the level of individual surface bonds can facilitate the rational development of chemical sensors based on these materials. A more detailed description of the effects of passivation on electronic properties follows in section V.A.

a. Sulfide Treatments

A variety of sulfide-based passivation treatments have been reported for GaAs.[4] Reagents employed include H_2S, Na_2S, $(NH_4)_2S_x$ ($x \geq 1$), SeS_2, and P_2S_5. Common characterization tools have included XPS and diffraction methods, with PL often used to quantify the impact of the passivation treatment.[57,63,105−116]

Collectively, these experiments yield evidence that the choice of passivant, its concentration, the duration and temperature of treatment, and the semiconductor carrier type and concentration can all affect the surface properties and hence the passivation quality. However, some trends common to most sulfide treatments are becoming apparent. It is generally agreed, for example, that at room temperature the sulfide-treated surface displays a (1 × 1) LEED pattern, which is transformed into a (2 × 1) pattern upon annealing.[33,116−120] The temperature at which this is reported to occur covers a range of 250−500 °C. The process may in fact occur gradually over a temperature range, as evidenced by LEED results reported by Wang and Weinberg for an $(NH_4)_2S_x$-treated surface; they observe the appearance of a weak (2 × 1) LEED pattern at 550 K, which is found to sharpen at 850 K.[117] The characteristic streaky appearance of the (2 × 1) LEED pattern has been noted by many researchers, suggesting a more complicated structure.

In an STM study comparing annealed $(NH_4)_2S_x$ and gaseous sulfur-treated GaAs (001) surfaces, Tsukamoto et al. found a (2 × 6) reconstruction for both surfaces.[121] However, whereas the gaseous sulfur-treated surface is uniform, the $(NH_4)_2S_x$-treated surface is highly irregular and composed of different regions of varying surface reconstructions, with (2 × 6) domains dominant. They attribute this difference to the etching effect of the aqueous sulfide treatment.

The precise structure generating the observed surface reconstruction has been the source of much debate. While early reports stressed the importance of As−S bonds at the surface, it has now become apparent that Ga−S bonds dominate.[33,111,113−115,119,120,122−125] In fact, it is agreed that annealing to temperatures above 400 °C exclusively favors Ga−S bonds at the surface.[33,111,116,119,125−128]

In a comparison of the Ga-rich (111) and As-rich (111) faces (the so-called A and B faces, respectively), Sugahara et al. deduce, based on AES sulfur-coverage analysis, that S is more strongly bound to Ga.[33] These observations are consistent with the fact that Ga−S bonds are thermodynamically more stable than As−S bonds.[18,116,129,130] Similar surface structural models have been proposed for both H_2S- and $(NH_4)_2S_x$-treated surfaces, as summarized in Figure 8.[17,111,117,122,126,127,131,132] For the sulfide-treated (001) surface displaying a (1 × 1) structure, Ohno et al., on the basis of pseudopotential calculations, predict that S resides in As vacancies and is bridge-bonded

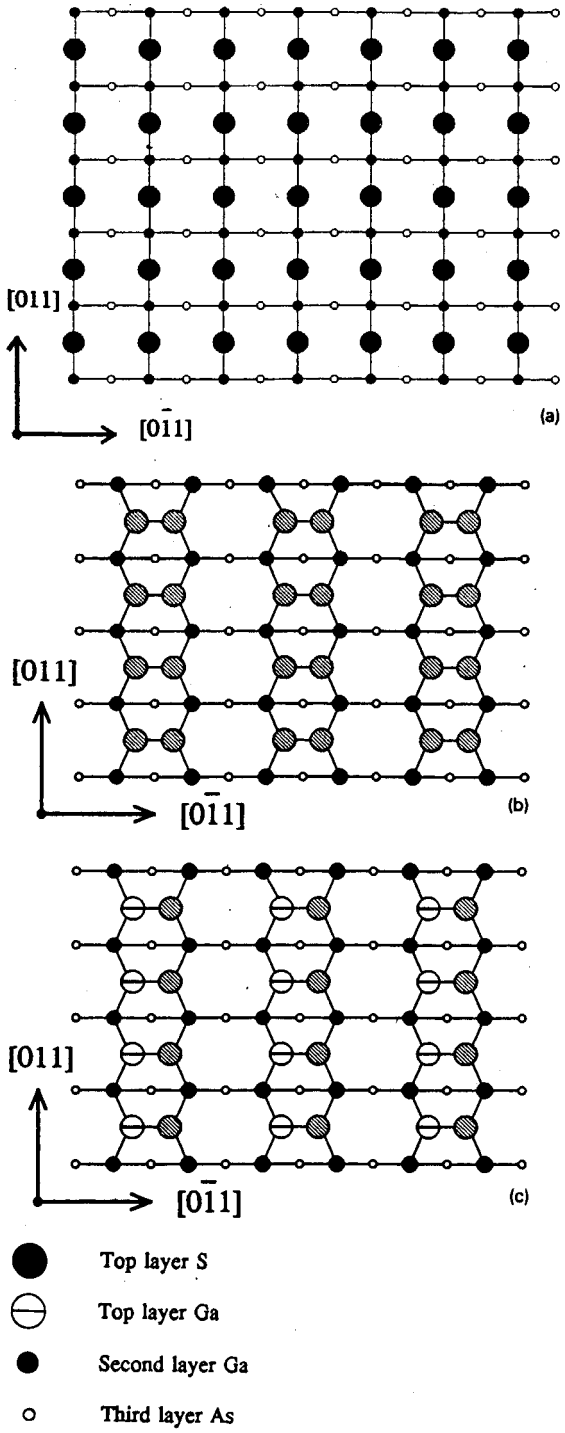

Figure 8. Possible surface structure models for sulfur on GaAs (100), where the atomic symbols are defined in the figure. In addition, crosshatched circles in parts b and c are sulfur atoms that are involved in surface dimer formation. (a) The bridge-bonded model, corresponding to a 1 × 1 structure with one monolayer of sulfur coverage; (b) the S−S dimer model, corresponding to a 2 × 1 structure with one monolayer of S coverage; (c) The S−Ga dimer model, corresponding to a 2 × 1 structure with a half monolayer of sulfur coverage. (Reprinted with permission from ref 134 and references therein. Copyright 1995 Elsevier Science.)

to surface Ga atoms.[17,130] Using PED, Lu and Graham provide compelling experimental evidence for this structure.[111]

Both S−S dimers and Ga−S dimers have been proposed as structural models for the (2 × 1) reconstruction.[111,117,127] Ohno found that S−S dimers are expected to be energetically stable.[17] Using RAS, Paget et al. observed such S−S dimers.[128] PES studies of the S core levels suggested the existence of S-dimers at the surface.[33,116] However, such a surface structure is not believed to be consistent with the observed improvement in electronic properties.[117] According to electron counting rules, such a surface, containing an odd number of electrons per (2 × 1) unit cell, should be metallic in nature, which implies poor electronic properties. As a solution to this apparent conflict, Wang and Weinberg proposed an alternate model involving Ga−S surface dimers, which predicts semiconducting behavior.[117]

Although different sulfide treatments appear to share many common characteristics, it should not be assumed that they are functionally interchangeable. The reactions differ in nature substantially, and unfortunately, studies addressing these differences are relatively few in number. Unlike most gaseous treatments, the passivants used in aqueous treatments, such as $(NH_4)_2S_x$ and Na_2S, also promote complicated etching reactions, affecting the semiconductor's surface morphology and usually the surface stoichiometry, as well.[57,133] Octadecylthiol (ODT) and H_2S treatments have both been reported to produce smoother, more uniform surfaces, whereas those from $(NH_4)_2S_x$ treatments have consistently been found to be highly irregular and nonuniform.[120,121] Moreover, etchant-dependent selective removal of surface atoms is suspected to occur.[57,133]

In a comparison of sulfide coverages obtained from H_2S and $(NH_4)_2S_x$ treatments of GaAs (100) surfaces using Rutherford backscattering and particle-induced X-ray emission, Xia et al. report a 2-fold difference, with coverages of 0.55 and 1.1 monolayers, respectively.[134] However, further sample treatment can conceivably influence these values. For example, Chung and Yi et al. found that on the GaAs (001) surface, at 100 K, dissociative adsorption of H_2S occurs, with hydrogen preferentially bound at As sites, as evidenced by HREELS.[47,48] According to TPD experiments, they find that AsH_3 and H_2S are liberated from the Ga-rich surface upon further annealing, leaving behind free Ga sites for further H_2S binding. After repeated annealing and H_2S exposure cycles, they claim, on the basis of AES coverage analysis, that the surface is completely passivated with sulfur, in contrast to the low coverage value reported above by Xia et al. for a sample that had undergone a single exposure.

b. Halogen Treatments

Simpson and Yarmoff published an excellent review of halogen reactions with III−V surfaces.[5] Molecular halogens are found to undergo dissociative adsorption on these surfaces, and subsequent surface reactions are sensitive to surface morphology, composition, and temperature. For Br_2 and Cl_2 on GaAs, the halogen adsorbs as either islands or 1-D chains for temperatures below 550 K, whereupon heating to above 625 K induces surface etching.[135,136]

Etching at room temperature has been observed for high surface coverages ($\sim 5 \times 10^4$ Langmuirs in the case of Cl_2).[5] Generally, both As and Ga are found to be highly reactive toward Cl_2, with Ga-rich surfaces typically demonstrating enhanced reactivity.

In a recent STM study, Liu and co-workers found that Br_2 prefers to bind to surface Ga, as demonstrated by its selective reaction with second layer Ga atoms exposed at defects on the As-rich GaAs (001)-2 × 4 surface.[137] This is shown in Figure 9. It is noteworthy that Br_2 reacts with Ga to the exclusion of the more readily accessible surface As dimers.

Adsorption of I_2 onto III−V surfaces, followed by subsequent annealing, has consistently been found to produce a surface terminated by group V atoms, irrespective of initial surface orientation and stoichiometry.[138] As for the other halogens, etching is also found to occur at room temperature upon exposure to excess I_2.[5] More recently, the reactions of alkyl halides with GaAs surfaces have begun to receive attention. In a study of etching reactions of ethyl iodide on the GaAs(100) surface, Singh et al. find that surface Ga atoms are selectively removed as GaI on the Ga-rich surface.[139] In contrast, the As-rich face is unaffected by ethyl iodide treatment.

c. Treatments with Other Molecular Adsorbates

In addition to sulfides and halogens, the interaction of GaAs with a variety of other species has been studied. These include metal alkyls, nitrogen-containing hydrides, amphiphilic molecules able to form self-assembled monolayers and Langmuir−Blodgett films, fullerenes, and clusters. In several cases, evidence for site-selective binding has been obtained, leading to customized surfaces that have considerable potential for chemical sensing.

A number of metal alkyls have been studied at GaAs surfaces owing to their importance in metal organic chemical vapor deposition (MOCVD) processes used in the growth of semiconductor thin films. Most commonly investigated have been the reactions on GaAs surfaces of trialkylgallium and dialkylzinc compounds used in the growth of GaAs and ZnSe overlayers, respectively.[140−142] In a study comparing the Ga-rich (4 × 2) and As-rich (2 × 4) and c(4 × 4) GaAs(100) surfaces for adsorption of diethylzinc, using HREELS and TPD, Lam et al. report that diethylzinc undergoes dissociative adsorption at room temperature on all three faces, forming surface ethyl and Zn as adsorbates. Surface Zn is found to desorb at 560 K on the Ga-rich surface and at 585 K on the As-rich surfaces, indicating that the Zn−As interaction is stronger.[141]

Exposure of GaAs to ammonia and hydrazine, which have relatively high sticking coefficients on the GaAs surface, leads to passivating films of GaN. For example, hydrazine can react at ~400 °C, extracting Ga from the surface of the substrate.[143,144] The insulating GaN layer that results serves to exclude both holes and electrons from the surface region.

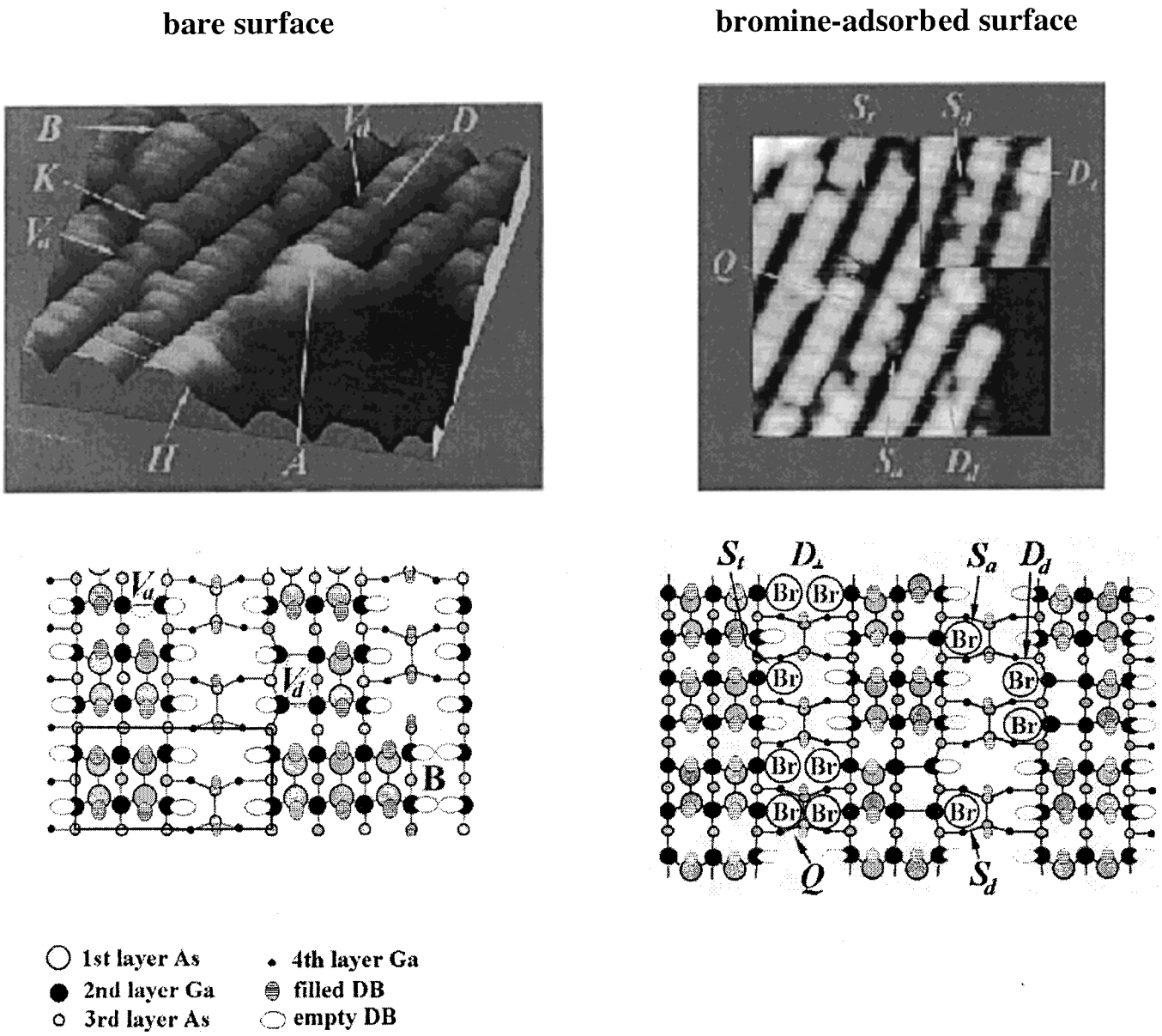

Figure 9. (Upper panels) Filled-state STM images of the bare arsenic-rich GaAs (001)−2 × 4 surface (left-hand panel); and the same surface dosed with bromine to give 0.4 monolayers of coverage (right-hand panel). (Lower panels) Corresponding schematic representations of the surface sites on the bare surface (left-hand panel) and the bonding structures of the adsorbed Br atoms at various Ga sites (right-hand panel). DB represents dangling bonds. Site labels are defined in the source of these images. (Reprinted with permission from ref 137. Copyright 1998 the American Physical Society.)

Self-assembled alkanethiol monolayers, which have been primarily studied on gold surfaces, have also been prepared on GaAs.[6,63] The thiols were presumed to bind selectively to arsenic atoms on the surface.[145,146] Figure 10 shows the proposed orientation of ODT on GaAs (100) based on IR experiments. Crooks and co-workers functionalized the unbound end of the thiol chain with carboxylic acid groups.[147] The acid-terminated self-assembled monolayers on gold were then demonstrated to sense basic analytes through changes in surface IR spectra and in mass.

Passivation of GaAs has also been attempted by adsorption of the amphiphilic molecule 22-tricosanoic acid, $CH_2{=}CH{-}(CH_2)_{20}{-}COOH$, following an initial photochemical unpinning treatment.[148] The authors propose that these films can serve as the basis for chemical sensors and other devices and that the use of polymerized films of similar molecules can lead not only to chemically sensitive surfaces but also to enhanced electronic properties. Langmuir−Blodgett films of hexadecanol have been observed by Rao and Kulkarni to improve the electronic properties of GaAs.[149] Langmuir−Blodgett films have also been used with a II−VI material. When 10,12-heptacosadiynoic acid was photopolymerized on $Hg_{1-x}Cd_xTe$, this polymer provided a conductive film on the surface that is claimed to prevent oxide growth for both n- and p-type $Hg_{1-x}Cd_xTe$.[150]

Films of C_{60} have been deposited on GaAs(001) to give highly surface-specific adsorption, as revealed by STM.[151] The 2 × 6 reconstruction, shown in the STM image of Figure 11, shows that the fullerenes cluster on the surface, eventually forming a (111) structure that has also been observed on other GaAs surfaces. The molecules adsorb in the troughs of the dimers rather than on step edges. The As-rich (001)

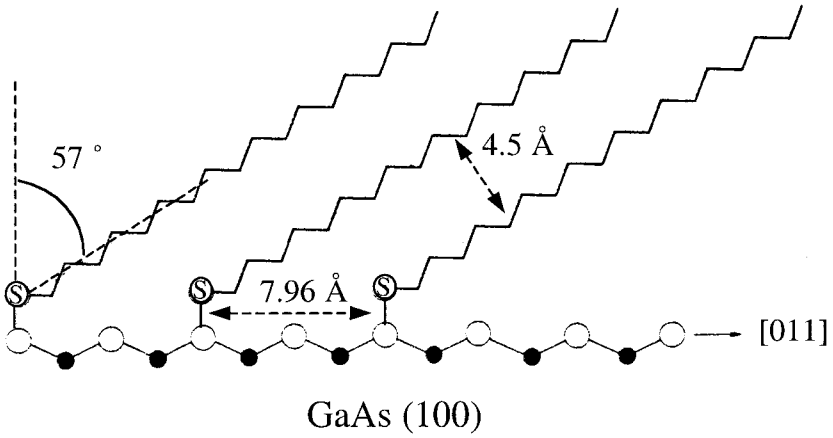

Figure 10. Side view of a possible monolayer structure of octadecylthiol on GaAs (100), assuming that the chains tilt along the [011] direction. Arsenic atoms are indicated by open circles and gallium atoms by filled circles. (Reprinted from ref 6 with permission from John Wiley & Sons, Inc.)

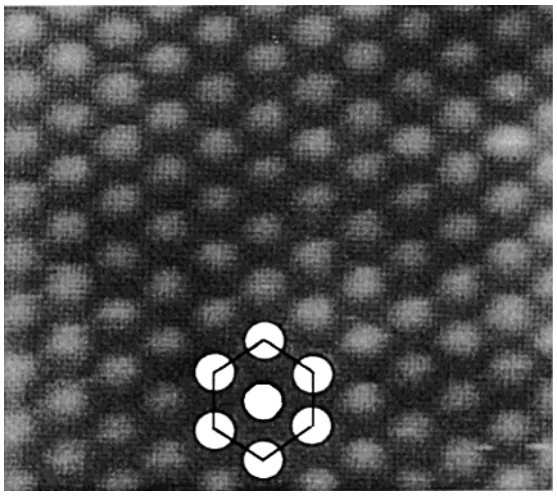

Figure 11. High-resolution STM image of a C_{60} multiple-layer film grown on the GaAs(001)−2 × 6 surface, 220 × 200 Å. (Reprinted with permission from ref 151. Copyright 1996 Elsevier Science.)

2 × 4 reconstruction leads to chains of C_{60} molecules running along the [110] direction, with ∼24 Å between each chain; with three layers adsorbed, an FCC (110) oriented film grows.

Another example of site-selective chemistry to prepare tailored surfaces, reported for II−VI semiconductors by Leung et al., is to exploit thermodynamically favored exchange reactions.[152] For example, limited exposure of CdSe to aqueous Ag^+ ions converts the surface to Ag_2Se:

$$CdSe\ (s) + 2Ag^+\ (aq) \rightarrow Ag_2Se\ (s) + Cd^{2+}\ (aq) \quad (11)$$

The presence of analytes such as aniline derivatives in toluene solution could be detected from PL responses. These responses were substantially larger than those recorded for the unexchanged CdSe surface, an effect that was interpreted in terms of an isotype Ag_2Se/CdSe heterojunction model.

Barron and co-workers devised a systematic method for designing tailored GaAs surfaces.[153] By compiling a list of Ga− Ga distances as a function of donor ligand for molecular bridge-bonded Ga compounds and comparing these values to Ga−Ga distances characteristic of GaAs surfaces, they can rationalize the strong surface affinities of certain donor ligands for the surface. Figure 12 summarizes Ga−Ga values for bridging donor ligands, along with the values found for GaAs and GaS surfaces.

To explore these relationships, Barron et al. synthesized and characterized carboxylate- and thiolate-bridged Ga dimers. In combination with data for higher oligomers obtained by others, they deduced that thiolate ligands should readily form strong bonds with GaAs and c-GaS surfaces, as the Ga−Ga separations are well-matched for the molecular and bulk species, with surface Ga−Ga distances of ∼3.9 and ∼5.6 Å for GaAs and c-GaS. In contrast, for the carboxylate-bridged species, the Ga−Ga separation does not overlap at all with the values found at the bulk surfaces, implying that considerable surface reconstruction is involved in binding such a ligand, posing an energetic barrier. Studies of these donor ligands at bulk surfaces will be good tests of the general applicability of this approach to the design of practical tailored surfaces.

V. Adsorbate Effects on Electronic Properties of III–V and II–VI Semiconductors

Many of the surface modification strategies discussed in the previous section were conducted with the goal of controlling the electronic properties of GaAs and CdSe. As the relationship of surface structure and composition to semiconductor electronic properties becomes better understood, adsorption-controlled sensor characteristics can become more easily customized to produce desired sensitivity, selectivity, kinetics, and robustness. In this section, these relationships are explored in more detail, again focusing on GaAs and CdSe as representatives of III−V and II−VI materials.

A. Surfaces of III–V Semiconductors

Given the importance of passivation (section IV.C), surface treatments that enhance the PL intensity of III−V semiconductors have received considerable attention. Many investigations have attempted to elucidate the mechanism by which surface modifica-

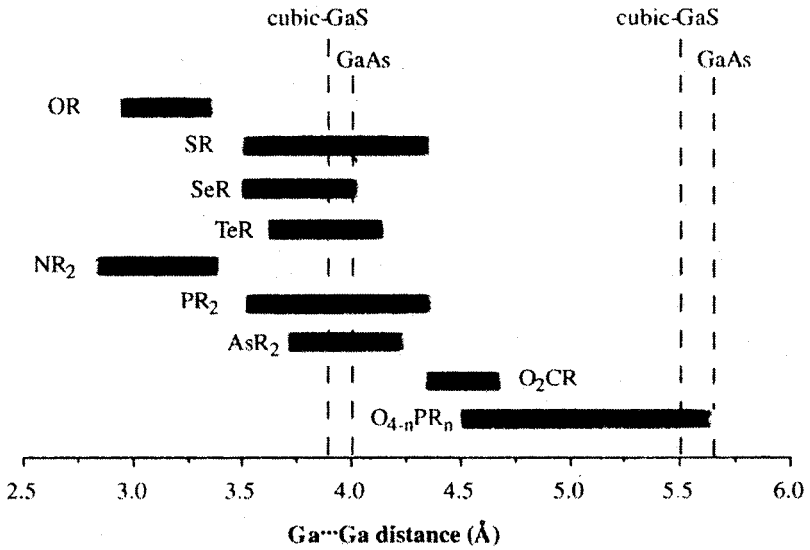

Figure 12. Correlation of Ga−Ga distances of adsorbing complexes with those of GaS and GaAs substrates. Bars represent the range of Ga−Ga distances in complexes of Ga dimers having the indicated bridging ligands. The dashed lines indicate nearest and next-nearest Ga−Ga distances on bulk cubic-GaS and GaAs surfaces. (Reprinted with permission from ref 153. Copyright 1998 Elsevier Science.)

tions occur and whether the treatment results in Fermi level unpinning. The literature is dominated by studies focusing on inorganic and organic sulfide treatments of the GaAs(100) surface. Summarized below are key results from over a decade of experimental and theoretical studies.

a. Inorganic Sulfides

Early studies of Na_2S and $(NH_4)_2S_x$ ($x \geq 1$) treatments were conducted in aqueous solution on n-GaAs(100) samples that had undergone a simple "dip and dry" procedure, with no further processing of the sulfide-coated surface.[62,107,108,110,113−116,154] An enhanced PL intensity was observed, accompanied by a reduction in the surface recombination velocity. Using Raman techniques, Sandroff et al. initially reported a decrease in band bending, as evidenced by a reduction in E_{fs}: from 0.78 eV for the air-oxidized, surface Fermi level-pinned value (near midgap) to 0.46 and 0.12 eV for Na_2S and $(NH_4)_2S$ treatments, respectively.[114] However, numerous studies using more direct methods, such as sample conductance, PES, and photoreflectance, appear to be in general agreement that the sulfide-treated surface before annealing actually exhibits increased band bending, with reports for the magnitude of the downward shift in E_{fs} ranging from 0.1 to 0.5 eV.[33,107,108,110,116,154−157]

Subsequent annealing of sulfide-treated n-GaAs surfaces has been shown to produce a decrease in band bending of not more than 0.3 eV from the sulfide-treated value for annealing temperatures at or above 360 °C.[33,156,158] At these elevated temperatures, PES studies have shown that only Ga−S bonds remain at the surface, suggesting that surface gallium atoms play an important role in GaAs passivation. Upon complete desorption of the sulfide overlayer at 650 °C, Arens et al. report that the band bending had been restored to that originally observed on the clean surface.[158]

In an extensive study, Paget et al. provide a correlation between the surface composition and such properties as the PL intensity and calculated surface recombination velocity during various annealing stages of an $(NH_4)_2S$-treated p-GaAs (100) surface.[156] Between 360 and 520 °C, according to Auger analysis, the surface becomes depleted in sulfur, with surface Ga dimers appearing based on RAS measurements, Figure 13. These changes in surface composition are accompanied by a concomitant decrease in PL intensity. Not shown in the figure is that over this temperature range, the position of the surface Fermi level is unaffected for this sample based on PR measurements. The diminution of the PL intensity was attributed to an increase in surface recombination velocity from the loss of adsorbed sulfur, as seen in Figure 13.

The effects of initial surface composition and reconstruction on the impact of the sulfide treatments are not clear. Using plasmon energy intensities from HREELS analyses, Arens et al. observed nearly identical band-bending behavior as a function of annealing temperature for the sulfur-coated As-rich (2 × 4) and Ga-rich (4 × 2) GaAs(100) surfaces.[158] In contrast, Moriarty et al. observed that band bending depended on annealing for the Ga-rich (4 × 2) surface but was insensitive to annealing for the As-rich (2 × 4) surface.[119] Additionally, Lunt et al. reported that the steady-state PL intensities of Na_2S-treated GaAs-(100) surfaces were independent of the initial surface composition obtained by using different etching protocols.[63] These apparent inconsistencies could likely be a consequence of different sulfur treatments used, as treatment-specific etching of the surface occurs for certain sulfidization reactions, as pointed out earlier in section IV.C.[57,63,133]

Yablonovitch et al. stressed that although Fermi level pinning implies the presence of a surface potential, residual band bending does not require that Fermi level pinning is present.[159] Many researchers have claimed that sulfide treatment merely

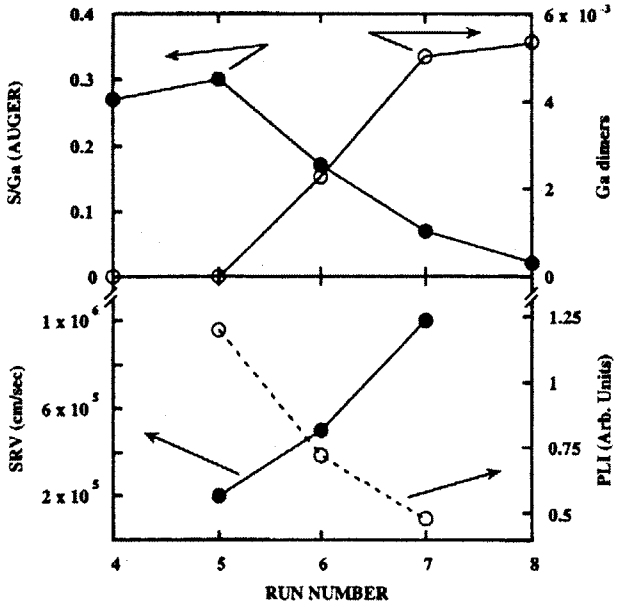

Figure 13. Effect of successive annealing (run number) on sulfur desorption and on the surface electronic properties of a GaAs (001) substrate. Run numbers 4−8 correspond to annealing temperatures 270, 360, and 520 °C and successive annealings at 520 °C, respectively. (Top panel) Magnitude of the S/Ga Auger signal (left-hand scale) and Ga dimer concentration, estimated from RAS (right-hand scale) with repeated annealings. (Bottom panel) Corresponding effects on the PL intensity (right-hand scale) and calculated surface recombination velocity (left-hand scale) caused by these annealing treatments. (Reprinted from ref 156 with permission from the American Physical Society, copyright 1996.)

re-pins the surface Fermi level at a new energy.[107,108,110,155,157] Since the real challenge in GaAs surface modification strategies is to unpin the Fermi level, Shen et al. recently noted the importance of determining both the band bending and the SDOS in order to assess the effectiveness of a treatment.[60]

Fermi level unpinning has been claimed for both $(NH_4)_2S$- and Na_2S-treated surfaces based on a reduction in SDOS inferred from the electronic performance (C−V and I−V curves) of MIS (metal−insulator−semiconductor) structures and from the observation of a metal-dependent Schottky barrier height.[109,160] However, a relatively minor reduction was reported in these studies, from $\sim 10^{13}$ cm^{-2} eV^{-1} for the untreated surface to $\sim 10^{12}$ cm^{-2} eV^{-1} for the sulfidized structures. Deep level transient spectroscopy (DLTS) on MIS structures using Na_2S- and $(NH_4)_2S$-treated n-GaAs(100) surfaces presented evidence for a reduction in density of the higher energy trap of the two deep levels present at $E_c = 0.58$ eV and $E_c = 1.15$ eV in as-grown GaAs.[157] The presence of a high density of states at the remaining trap level re-pins E_{fs} closer to the valence band edge and is proposed to be the origin of the increase in band bending. Hasegawa's PL-based method of surface state spectroscopy has shown that sulfide treatment does not lead to a significant change in the SDOS. Instead, based on theoretical modeling, a negative fixed surface charge for n-GaAs is proposed, possibly from ionic species present in the overlying film, to account for the observed increase in band bending.[62,107,108]

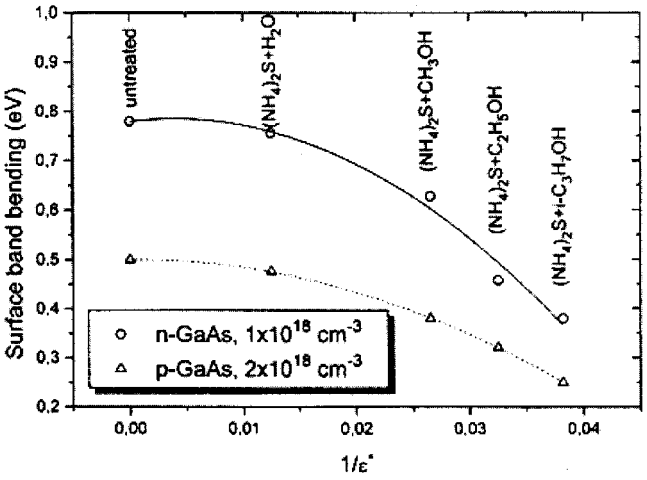

Figure 14. Dependence of the surface band bending for n-GaAs and p-GaAs substrates versus the reciprocal effective dielectric constant of the ammonium sulfide solution used to passivate the semiconductor surface. (Reprinted with permission from ref 165. Copyright 1998 Elsevier Science.)

Unlike the aqueous sulfide treatments discussed above, a significant reduction in the SDOS relative to the untreated surface was recently found to be induced by a H_2S plasma treatment. From PR measurements, a nearly 1000-fold reduction in surface state density was found: $\sim 3 \times 10^{13}$ cm^{-2} eV^{-1} for the untreated surface compared to 6×10^{10} cm^{-2} eV^{-1} upon sulfidization.[60]

Bessolov et al. studied the effects on band bending of a systematic variation in the chemical properties of the surface treatment and of the semiconductor's carrier properties.[161−165] The solution dielectric constant has been shown to be an important factor influencing the magnitude of the shift in E_{fs} resulting from sulfide treatment.[161,165] By use of a series of alkyl alcohols to tune systematically the dielectric constant, ϵ, of the $(NH_4)_2S$ solution, the efficacy of the sulfide treatment was found to improve in low dielectric solvents. These results, reproduced in Figure 14 and obtained through CPD and Raman measurements for GaAs, demonstrate that band bending decreases for both n- and p-GaAs with increasing $1/\epsilon$; the work function also increases for both samples with increasing $1/\epsilon$. These results can be partially understood as an enhanced affinity of the ionic sulfide species for the more polar GaAs surface in low dielectric solvents.

In a separate study, Bessolov et al. varied the initial work function, $\phi_{w,0}$, of the untreated GaAs substrate by using a wide range of doping levels (10^{15}−10^{19} cm^{-3}) while using the same Na_2S solution for the treatment.[162−164] The resulting change in work function was found to vary linearly with the quantity $(\phi_{w,0} - \phi_{w,0}^c)$, where $\phi_{w,0}^c$ is called the characteristic work function, corresponding to the value of $\phi_{w,0}$ that is unaffected by sulfide treatment. The authors reason that for $\phi_{w,0}^c$, the electronegativity of the semiconductor (see section II) matches that of the reacting sulfide ion in solution; as for molecular systems, no net transfer of charge occurs upon reaction of two species that are matched in electro-

negativity, accounting for the behavior of samples with work function $\phi_{w,0}$[c].

To summarize this section on sulfide treatments, it appears that they can shift the surface Fermi level toward the flatband condition after annealing; however, the Fermi level does not seem to be unpinned by these treatments. In striking contrast, H_2S seems to reduce the SDOS substantially.

A promising surface treatment reported by Tabib-Azar et al. is to deposit a metastable cubic phase of GaS, which is nearly lattice-matched to GaAs, using a cubane precursor $[(t\text{-Bu})GaS]_4$.[166] A roughly 100-fold increase in PL intensity was observed and found to persist over an extended period of at least 6 weeks. From C−V curves of MIS structures based on these materials, they find a reduction in interface state density, suggesting that such a treatment might unpin the surface Fermi level.

b. Organic Sulfides

The poor oxidative stability of the Na_2S- and $(NH_4)_2S$-treated surfaces, leading to rapid degradation of electrical properties, has prompted interest in organic sulfides, particularly long-chain thiols. The hydrophobic alkyl chains are expected to act as a barrier, preventing oxygen and water from reaching and reacting with the semiconductor surface. Most observations have supported this expectation: Instead of improvements with inorganic sulfide treatments that lasted only hours or days, improvements lasted weeks or months with organic sulfide treatments.[167,168]

Surprisingly, very few studies have investigated in detail the effects of ODT treatment on GaAs electrical properties. An increased barrier height has been noted in Schottky diodes.[146,169] Nakagawa et al. report an approximately linear dependence of the Schottky barrier height on thiol alkyl chain length, increasing to a maximum value of about 0.05 eV relative to the untreated surface for chains containing 20 carbon atoms.[146] Contrary to these electrical measurements, Dorsten et al. found a 25% reduction in the depletion region based on Raman spectroscopy, corresponding to a decreased surface potential.[168] From diode C−V and I−V characteristics, Remashan et al. deduce that ODT treatment causes a 10-fold reduction in the SDOS in the upper half of the band gap; however, a minimum value of $\sim 10^{12}$ cm^{-2} eV^{-1} is estimated to remain at midgap, leaving the Fermi level pinned.[169]

Other organic sulfides that have been examined include dithiocarbamate, (3-mercaptopropyl)trimethoxysilane, and plasma-polymerized polythiophene.[61,167,170] The polythiophene treatment has been reported to eliminate the higher energy trap level of the two identified on the untreated GaAs (110) surface.[61]

Lunt et al. conducted one of the few systematic studies of a broad range of organic thiols. These compounds were found to produce an increase in PL intensity, as summarized in Figure 15.[63,112] Lunt et al. observe that the efficacy of the sulfide treatment parallels trends in binding constants of sulfide ligands

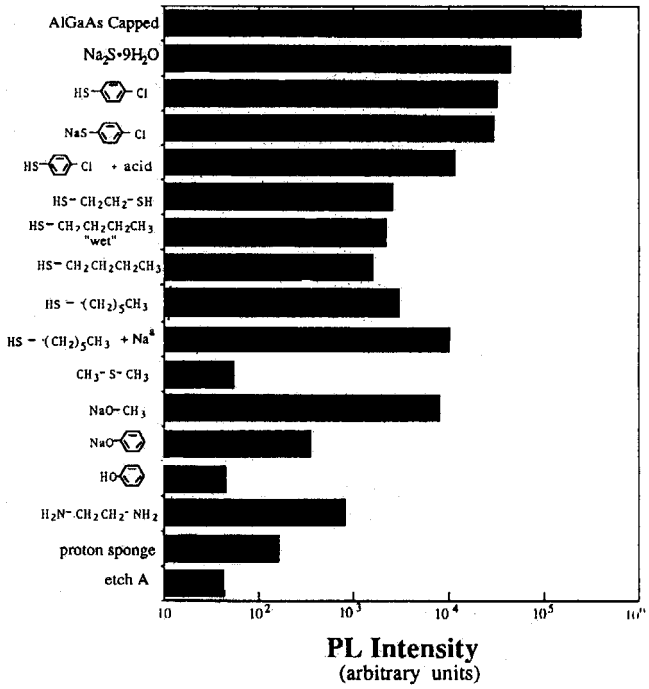

[a] Solvent was tetrahydrofuran.

Figure 15. Bar graph of steady-state PL intensity at 874 nm for 1.0-μm-thick epilayer (100) n-GaAs samples after exposure to various nonaqueous solutions. For the highest PL intensity sample, the term "AlGaAs capped" refers to a structure whose terminating topmost layer has a composition of $Al_{0.4}Ga_{0.6}As$. Additional experimental details are given in ref 63, from which this graph is reprinted.

toward Lewis acidic transition metal centers, which they believe indicates that specific coordination interactions at the surface are important. This is also supported by results from another study, in which the same authors found that adsorption from aqueous solution of the anionic species CN^- and SCN^- did not influence the PL intensity of the GaAs substrate, indicating that electrostatic effects are insufficient to produce a change in PL behavior.[63] Furthermore, soft sulfur donors generally appear to be more effective than hard oxygen donors in producing a change in PL intensity (Figure 15). On the basis of hard−soft/acid−base theory and assuming similar coverages, this observation suggests that the active surface sites are polarizable and electron deficient in chemical character. From time-resolved PL studies at high excitation intensities, both inorganic and organic sulfides were generally found to cause a substantial reduction in surface recombination velocity. In contrast, methoxide ion had no effect on the surface recombination velocity and was inferred to enhance PL intensity by affecting band bending.

Bastide et al. systematically studied a class of oxygen-donor ligands, benzoic acid derivatives, as adsorbates on GaAs and found that they could be used to control the semiconductor's work function.[171] The direction and magnitudes of the work function changes were correlated with the dipole moments of the adsorbates. By IR spectroscopy, the acids were found to bind as carboxylates through coordination to oxidized surface Ga or As atoms, with about a monolayer of surface coverage. CPD measurements

indicate that the adsorbate influences the electron affinity, with little effect on band bending.

c. Selenides

Given the polarizable, electron-deficient nature of binding sites on GaAs inferred by Lunt et al., the effectiveness of chalcogenide-induced modification of GaAs electronic properties might be expected to follow the trend O < S < Se.[63,112] Numerous studies of Se-based treatments appear to be in accord with this hypothesis, with studies of Se adsorption reporting a substantial reduction in band bending to ~0.1 eV, approaching the flatband condition.[172−174]

The S- and Se-based treatments share many similarities in chemistry at the GaAs surface. For example, treatment at elevated temperatures (>300 °C) shifts the preference from As−Se bonding at room temperature to surface Ga−Se bonding. This change in surface structure appears to be correlated with a substantial reduction in band bending.[174−178] The interfacial chemistry is reportedly similar for the Ga- and As-rich GaAs (111) surfaces and the (100) surface, with selenium uptake varying, however, according to (111)Ga > (100) > (111)As.[176]

Combined selenium and sulfur treatments have become popular, particularly use of SeS_2, in an effort to exploit the beneficial effects of both kinds of atoms.[173,179−185] Kuruvilla et al. identified a correlation between film thickness and PL efficiency, with the thinnest SeS_2 films producing the greatest PL intensities.[179−181] On the basis of AFM studies, they attribute this observation to the existence of a well-ordered (1 × 1) adlayer, with a lattice period of 3.8 Å on the GaAs (100) surface. This value is close to that of ~4 Å for the unreconstructed surface, and the nearly matched lattice parameters may be related to energetic stabilization of the GaAs surface through surface structural modification.

Related to this is an UHV−STM study by Pashley et al. of the n-GaAs (100) surface treated with elemental Se.[173] Evidence is provided for Se-induced removal of kinks in the dimer vacancy rows of the GaAs(100)−(2 × 4) surface. Surface states arising from such kinks are believed to contribute to Fermi level pinning on the (100) surface of n-type material.

High-resolution core-level photoemission spectroscopy excited with synchrotron radiation was used to study n-type GaAs (100) surfaces that were passivated at room temperature from CS_2 solutions of SeS_2.[184] Surfaces treated in this way had a chemically stratified structure of several atomic layers thickness. The surface is terminated with S−S bonds, beneath which are arsenic-based sulfides and selenides, which lie atop gallium-based selenides that are adjacent to the bulk GaAs substrate, as shown in idealized form below. Arsenic-based species were removed at low annealing temperature with little shift in E_{fs}, while gallium-based selenides were shown to provide the surface electronic passivation.

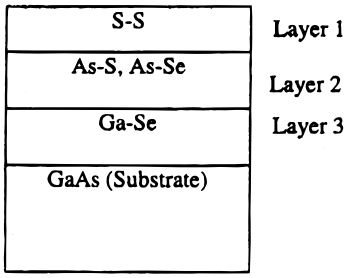

B. Surfaces of II–VI Semiconductors

a. General PL Properties

One of the principal methods for assessing adsorbate interactions with II−VI semiconductor surfaces has been to monitor steady-state PL intensities at low injection levels. Many of these studies have been conducted with single-crystal samples of CdS and CdSe. The PL response to a broad range of analytes has been found to define a "luminescent litmus test": Lewis bases and acids cause PL enhancements and quenching, respectively, relative to a reference ambient of either nitrogen or vacuum for gas-phase studies or pure solvent for solution studies. As will be shown in this section, the ready reversibility of many of these responses has permitted analytes spanning much of the periodic table to be examined.

Figure 16 illustrates the reversible PL response of CdSe to the Lewis base ammonia that in principle permits on-line analyte detection.[186] Models for interpreting the magnitude and concentration dependence of the PL response have been investigated. Rives reported on an attempt to model the ammonia−CdSe interaction computationally.[187] More recently, Geisz et al. used a finite element method (FEM) model incorporating the full range of carrier generation, transport, and recombination processes described in section II.C to identify conditions under which the dead-layer model should and should not work.[27,28,188] The results, shown in Figure 17, illustrate the combinations of electric field conditions and surface recombination velocities over which accord with the dead-layer model is expected. Many of the CdSe results reported below employed single-crystal samples with $n \approx 10^{15}$ cm^{-3}. The good fits to the dead-layer model observed suggest that a high surface recombination velocity is produced by the etching conditions employed. A similar FEM analysis has been reported for GaAs-based heterostructures.[28]

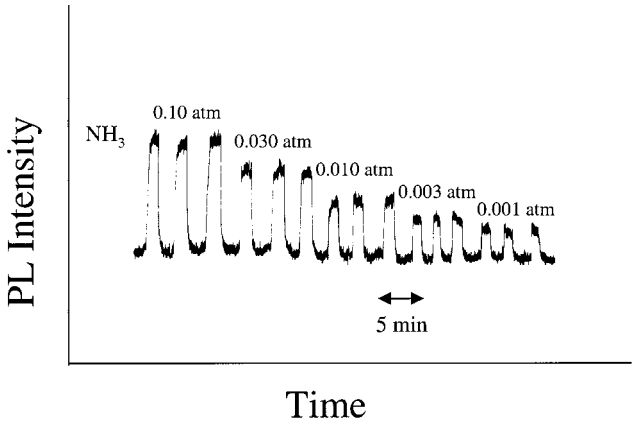

Figure 16. Changes in PL intensity at the emission band maximum resulting from alternating exposure of an etched n-CdSe sample to nitrogen (initial response) and the indicated partial pressures of ammonia in a nitrogen/ammonia mixed flow. (Adapted from ref 186.)

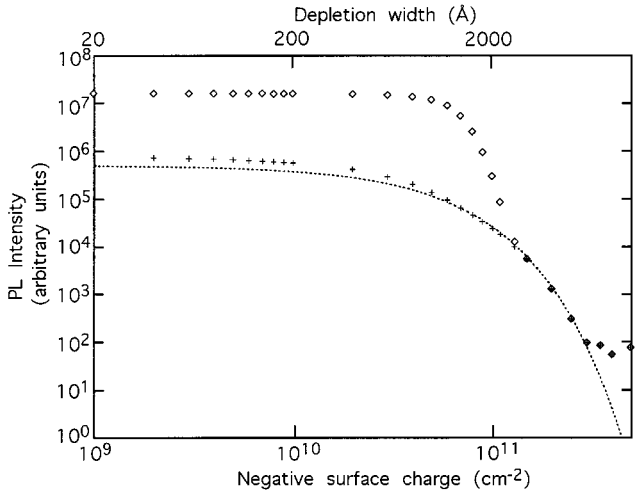

Figure 17. PL intensity calculated with a FEM model as a function of negative surface charge and depletion width for n-CdSe (5×10^{15} cm^{-3}) under conditions of low-level injection from 514 nm optical excitation. The dashed line is the curve predicted using the dead-layer model; the data points are FEM model predictions with a surface recombination velocity of 10^2 cm/s (diamonds) and 10^5 cm/s (plus signs). (Adapted from ref 188.)

For many of the systems examined, the concentration dependence of adduct-induced PL changes yields good fits to the Langmuir adsorption isotherm model, making it possible to obtain estimates of binding constants between the analytes and the surface. The quantitative form of the Langmuir adsorption isotherm model for monodentate or chelating binding is represented by[189]

$$\theta = [(KC)/(1 + KC)] \text{ or } 1/\theta = (1/KC) + 1 \quad (12)$$

Here, θ represents the fractional surface coverage, K is the equilibrium constant for binding the analyte to the surface, and C is the molar concentration of the analyte. The PL intensity in the reference ambient, PL_{ref}, corresponds to $\theta = 0$, and the maximum change in PL intensity, PL_{sat}, is assumed to correspond to $\theta = 1$. When these interactions have fit the dead-layer model (eq 5), intermediate values for θ have been estimated as the fractional change in dead-layer thickness:

$$\theta = \{\ln[PL_{ref}/PL_x]\}/\{\ln[PL_{ref}/PL_{sat}]\} \quad (13)$$

Occasionally the analyte PL responses do not fit the dead-layer model, presumably because of substantial adsorbate-induced changes in surface recombination velocity. Under these circumstances, values of θ have been calculated simply as PL ratios, PL_{ref}/PL_x. When these two methods have been directly compared, the extracted values of K have generally been within a factor of 2 of one another with those calculated from dead-layer changes larger.[190] Sample-to-sample variations in values of K for binding a particular analyte have been reported to span one-half an order of magnitude routinely, making order-of-magnitude comparisons of analyte effects most realistic.

Given the assumptions of the Langmuir model[189]—identical binding sites with the same enthalpy of adsorption and the absence of inter-adsorbate interactions—it is surprising that good fits are obtained. Most of the reported studies have been conducted with samples prepared by wet etching with bromine/methanol solution and subsequent exposure to air and moisture, which, from the results described in section IV.A, likely leads to highly inhomogeneous surfaces.

A summary of representative order-of-magnitude binding constants for adsorbates binding to the (0001) CdSe surface, as monitored by PL, is provided in Table 1, along with a description of whether adsorption caused enhancement or quenching of PL intensity. Although the table focuses on CdSe, similar effects have been reported for CdS and Te-doped CdS, CdS:Te (a more highly emissive material), when comparisons were made with CdSe. In one study of 32 carbonyl adsorbates, for example, essentially the same values of K were found for CdS:Te and CdSe substrates within experimental error.[191] Surprisingly, direct comparisons of the (0001) and less highly emissive, opposing chalcogenide-rich (000$\bar{1}$) face have been made for fullerene and 7,7,8,8-tetracyanoquinodimethane (TCNQ) derivative adsorbates and yielded similar binding constants.[192,193] Brief descriptions of the reported PL studies and related studies are presented below, organized based on the position in the periodic table of the likely ligating atom of the analyte.

An important caveat in making comparisons within and between adsorbate families is that absolute coverages are not known, limiting the ability to draw conclusions from relative PL changes. Acquisition of data on absolute coverage and the kind of sites occupied by adsorbates is needed to better understand the observations described below.

In addition to steady-state PL measurements, there have been several time-resolved PL studies reported, generally for CdS and CdSe exposed to aqueous chalcogenide solutions used to stabilize these materials as photoelectrodes. Adsorption of alkali metal and transition metal cations have also been investigated. Many of these adsorbates lead to substantial and often irreversible changes in surface recombination velocity that would be unsuitable for on-line chemical sensing and thus will not be discussed further.[64,65,67]

b. Group III Adsorbates.

Gas-phase adsorption studies involving group III compounds have been reported and emphasize the potential use of this methodology for detection of precursor gases used in the growth of materials by chemical vapor deposition (CVD; see section VI). As expected for Lewis acids, adsorption of a family of boranes caused quenching of CdSe PL relative to the reference intensity in a vacuum.[194] The quenching order—BF_3 > $MeBBr_2$ > Me_2BBr > Et_3B—could reflect increased steric demands and/or reduced Lewis acidity along the series. All of the adsorbate responses were well fit by the dead-layer model.

Surprisingly, the Lewis acidic trialkyl complexes Me_3Al, Me_3Ga, Et_3Ga, and Me_3In gave large (3−100-fold) irreversible PL enhancements relative to vacuum that appear to be caused by changes in surface

recombination velocity, as only poor dead-layer fits were obtained.[195] Irreversible surface chemistry was inferred to have taken place from these results. However, subsequent exposure of the surface to gaseous butylamine isomers was found to partially reverse the PL response, presumably through adduct formation with a group III atom-derived, surface-confined species; the magnitude of the recovery varied from 10% to 80% and was greatest with the least bulky amines and with Al and Ga. Completely reversible PL enhancements were obtained with discrete 1:1 adducts of Me_3Al:Me_3N and Me_3Ga:Me_3N. Here too, though, the PL responses were not in accord with the dead-layer model.

c. Group IV Adsorbates

A variety of unsaturated and Si-containing analytes have been studied on CdSe substrates. Meyer et al. reported PL enhancements in accord with the dead-layer model for CdS(e) surfaces exposed to a family of gaseous butenes.[196] These responses followed the trend 1,3-butadiene > *cis*-2-butene ≈ *trans*-2-butene > isobutylene ≈ 1-butene > *n*-butane, which, from left to right, is the order of increasing ionization potentials and thus poorer electron-donor character. PL enhancements were observed with allene, acetylene, and propyne, suggesting that these compounds, too, can donate π electron density to the semiconductor substrate.

Strongly π-acidic adsorbates such as TCNQ and several ring-substituted derivatives have been studied in dichloromethane. As expected, these compounds quench the PL of CdSe and give good fits to the dead-layer model.[192] The magnitude of the PL response was found to correlate with electrochemical reduction potential and could be detected for some derivatives at submicromolar concentrations. PL quenching was more substantial with the (0001) face relative to the $(000\bar{1})$ face, but similar binding constants were observed for both faces, suggesting that common binding sites are employed.

Zhang et al. found that toluene solutions of fullerenes, specifically C_{60} and C_{70}, also behave as π-acids and quench the PL of CdS(e) reversibly.[193] The responses for C_{60} fit the dead-layer model, but C_{70} could not be tested for adherence to the model because of interfering solution absorption effects. A competition experiment demonstrated that the surface has a preference for C_{70} over C_{60}, as shown in Figure 18.

Waldeck et al. studied single-crystal CdSe surfaces exposed to toluene solutions of chlorosilanes and found that when removed from solution, the semiconductor's PL decay time had lengthened irreversibly.[197] Surface recombination velocities were extracted from the data and were found to be in the order $Me_2(OMe)SiCl \geq PhMe_2SiCl > Me_3SiCl \geq$ untreated $> Me_2SiCl_2 > MeSiCl_3$, which was correlated with a corresponding decline in ionization potential along this series. The authors proposed that the chlorine atoms on the molecules react with the environment or the substrate, leaving the remaining silane fragment to polymerize on the surface. Mott−Schottky plots ($1/C^2$ vs bias voltage) demonstrated

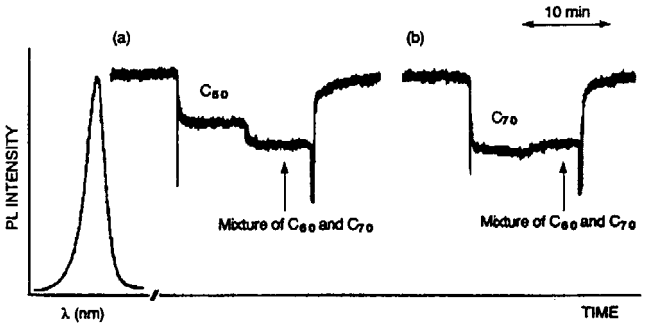

Figure 18. Competition adsorption experiment between C_{60} and C_{70} in toluene solution, based on fullerene-induced PL changes (monitored at ~710 nm) of an etched, single-crystal n-CdSe sample whose (0001) face is exposed to the solution. The left-hand edge of the figure shows the initial PL spectrum in pure toluene. Subsequently, (a) a C_{60} toluene solution is introduced into the sample cell, followed by an equal volume of a C_{70} toluene solution, resulting in a 1:1 molar mixture of the two fullerenes. The experiment is then repeated (b) with the opposite order of addition. The excitation wavelength is 632.8 nm throughout the experiment. (Reprinted from ref 193.)

that little to no modification of the depletion region results from this treatment.

Brainard et al. studied gas-phase adsorption onto CdSe of the chlorosilanes, H_2SiCl_2 and $HSiCl_3$. After an initial exposure to these compounds that gave an irreversible PL enhancement under steady-state conditions, subsequent exposures gave reversible PL quenching. These results did not fit the dead-layer model, which likely indicates a significant change in surface recombination velocity, in accord with Waldeck's findings.[197,198]

Brainard et al. also used PL to probe the interactions of (0001) CdSe surfaces with the vapors of the complete family of nine silapentane isomers, some of which have potential applications to CVD growth.[198] Observed PL responses under steady-state conditions were enhancements, and the source of Lewis basicity was proposed to be Si−H hydridic bonds. With the exception of *tert*-butylsilane, the magnitude of the PL response generally increased with the number of Si−H bonds.

d. Group V Adsorbates

Adsorption onto CdSe of a variety of amines and other species with group V donor atoms has been studied in the gas and solution phases. Meyer et al. found PL enhancements in the following order for gas-phase amines $NF_3 < NH_3$, $ND_3 < CH_3NH_2 < (CH_3)_2NH > (CH_3)_3N$ with PL changes fitting the dead-layer model for etched samples.[186] With the exception of Me_3N, whose interaction may be inhibited by steric effects, these PL changes correlate well with proton affinities: The more basic the amine, the greater the observed response.

Samples of CdSe that were freshly cleaved along the *c*-axis were found to give the same ordering of PL response toward the aforementioned amines, but the baseline PL intensity was much higher and the analyte responses typically did not fit the dead-layer model, suggesting that adsorption principally affects surface recombination velocity.[186] To investigate this effect in more detail, Leung et al. studied PL decay

times in the presence of amines.[66] The PL traces were fit to the Kohlrausch equation:

$$I(t) = I_0 \exp[-(t/\tau)^{\beta}] \quad (14)$$

β reflects and varies inversely with the distribution width of a set of exponential decay times, and the lifetime τ reflects the peak of the distribution. For the cleaved samples, adsorption of ammonia and methylamine were found to increase both β and τ relative to their values in the nitrogen reference ambient employed and support the notion that recombination kinetics are substantially affected by adsorption. The magnitude of the effect was found to decrease with increasing light intensity, which may reflect accentuated contributions of bulk properties as the depletion width is reduced.

Adsorption of a trio of group V CVD precursor compounds—ammonia, phosphine, and arsine—was compared on etched CdSe substrates using hydrogen, a commonly used carrier gas in CVD reactions, as the reference ambient.[199] All three hydrides gave PL enhancements on CdSe, consistent with their acting as Lewis bases toward the surface. The authors calculated that the reduction in the amount of trapped negative surface charge caused by adsorption (corresponding to the estimated reduction in depletion width using the dead-layer model) was on the order of 10^{10} cm^{-2}. This value would correspond to only about 0.01% of the possible Cd surface sites occupied by adsorbed species, if it is assumed that each adsorbed molecule frees one electron from the surface. The same study also investigated the effect of an increase in temperature on the PL response. Although raising the temperature substantially shortened adsorption and desorption times, a desirable outcome for reducing the response time in on-line detection schemes, there was a 3-fold reduction in PL intensity, representing a significant compromise in signal-to-noise ratio.

Evidence for the ability to tune electronic contributions to surface binding through substituent effects was reported from studies of the adsorption of a family of aniline derivatives from toluene solution onto CdSe and CdS.[200] The magnitude of the PL response was well fit by a Hammett plot, as shown in Figure 19, whose range spanned substantial PL enhancements, caused by electron-donating substituents such as *p*-methoxy, to slight quenching of PL intensity, caused by the highly electron-withdrawing *p*-cyano substituent. Time-resolved PL studies revealed no significant change in the PL decay profile between the reference toluene ambient and that of a toluene solution of *p*-methoxyaniline, suggesting that adsorption was principally modulating the PL intensity through depletion width effects.

Several aniline derivatives have also been studied on CdSe by Bruening et al., using a combination of Kelvin probe and photoexcitation techniques to determine adsorbate-induced effects on electron affinity and band bending.[201] Adsorption appears to affect principally the electron affinity of the samples rather than the band bending. While this appears to contradict the results obtained by Murphy et al., Bruening et al. suggest that the experimental conditions of air vs solution may account for the difference.[200]

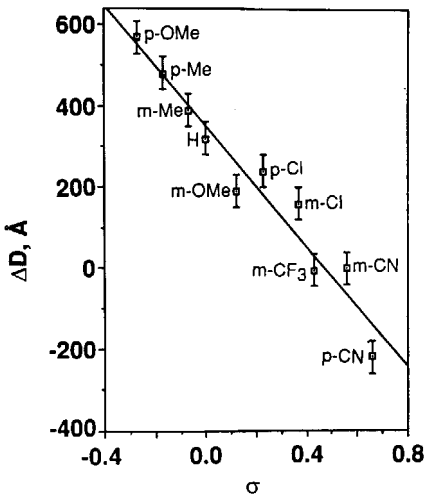

Figure 19. Plot of the maximum change in dead-layer thickness, ΔD, obtained for each aniline derivative from PL changes in toluene solution vs its Hammett substituent constant, σ. Positive values of ΔD correspond to a reduction in dead-layer thickness. (Reprinted from ref 200.)

As noted above in section IV.C, CdSe surfaces can be exchanged with aqueous silver ions to yield surface islands of Ag_2Se.[152] Leung et al. found that the binding constant for *p*-methoxyaniline was roughly twice that for an unexchanged CdSe surface on the same sample. There is, however, a tradeoff in the use of this treatment, as the PL intensity is significantly reduced by the exchange reaction.

Evidence for steric effects on binding has been provided by studies of chelation at the CdS and CdSe surfaces using diamines such as ethylenediamine and *o*-phenylenediamine adsorbed from cyclohexane solution.[190] Binding constants for these molecules are about 2 orders of magnitude larger than those obtained for sterically matched monodentate amines (see Table 1). The smaller reductions in dead-layer thickness estimated for chelating molecules was ascribed to smaller absolute coverages that might be expected for the more sterically demanding binding requirements of the chelate. Evidence for chelation of diphosphines was sought, but PL data were most consistent with a combination of bridging and monodentate binding modes.[202]

e. Group VI Adsorbates

A considerable number of adsorption studies have been conducted with carbonyl, phosphine oxide, and sulfide adsorbates on CdS and CdSe substrates. Nearly three dozen ketones and aldehydes were found by Kepler et al. to cause reversible PL quenching in accord with the dead-layer model in cyclohexane solution, indicating that these species act like Lewis acids toward the surface.[191] Binding constants, spanning roughly 4 orders of magnitude, from 10^1 to 10^5 M^{-1}, were enhanced by substitution of phenyl groups for methyl substituents. Hammett plots were consistent with stabilization of surface adducts by electron-withdrawing substituents. The largest binding constants were observed for α-diketones and quinones.

Cahen and Shanzer et al. used families of benzoic acids and hydroxamic acids to demonstrate that the electron affinity of CdSe and CdTe substrates can be controlled independently of band bending.[201,203] Using

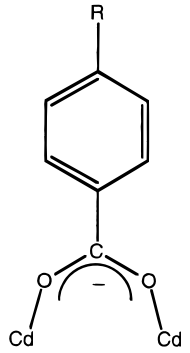

ATR-FTIR spectroscopy, they observed that benzoic acids bind preferentially to Cd sites on CdTe, probably in a bridging binding mode, as shown above; hydroxamic acids also bind to Cd, although their ligating mode was difficult to determine. Adsorption leads to changes in the work function for these materials that have been correlated to adsorbate dipole moments and to Hammett parameters. Data for intrinsic CdTe are shown in Figure 20, and

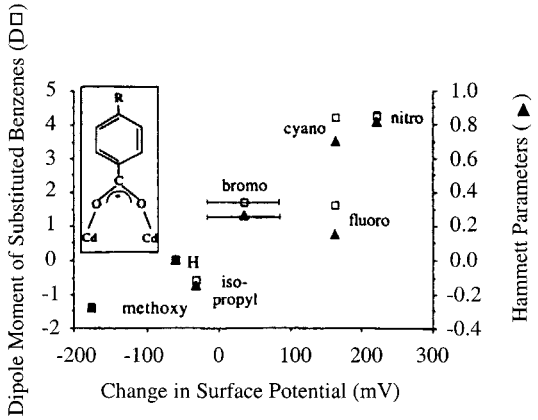

Figure 20. Change in surface potential of an intrinsic CdTe single crystal with adsorbed, substituted benzoic acids, as a function of adsorbate Hammett parameter (right-hand scale) and dipole moment (left-hand scale). (Reprinted from ref 203.)

similar results were found with single crystals of n-CdTe.

More recently, these researchers have taken such "band edge engineering" experiments a step further by using irreversibly bound dicarboxylic acid adsorbates such as those shown below in conjunction with several II−VI and III−V semiconductors.[204−207] As an example, using various derivatives of these adsorbates, systematic variations in both electron affinity and band bending were obtained on n-CdTe substrates. Additional characterization for these systems has been reported using two-photon photoemission spectroscopy.[208]

As part of their studies, Bruening et al. examined the effects of common etching procedures on the work function of CdSe.[201] They observed that the bromine/methanol etch increases the work function while a subsequent hydrazine treatment then reduces it.

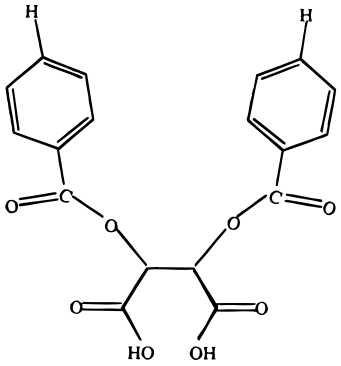

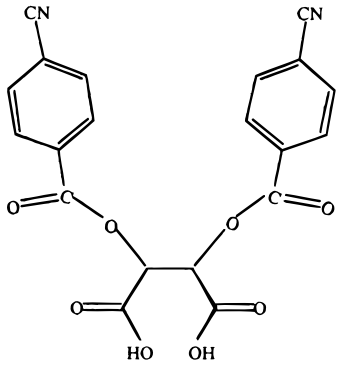

Because the bromine/methanol etch leaves an elemental Se residue on the surface, the authors suggest that the higher work function of Se relative to CdSe may account for the increase in work function. They note that such etching effects lead to irreproducible surfaces and can produce substantial variations in adsorption properties.

An oxygen-containing adsorbate that has been used extensively in the preparation of II−VI nanocrystals is tri-*n*-octylphosphine oxide (TOPO). Studies of the adsorption of this molecule onto single-crystal CdSe from toluene solution were reported by Lorenz et al. and illustrate the ability to probe solution aggregration phenomena with the PL methodology.[209] With either etched (0001), (000$\bar{1}$), or (11$\bar{2}$0) faces, a reversal of PL signature was consistently found at ∼10 mM TOPO concentration. Initially, at micromolar concentrations, reversible increases in PL intensity are seen, consistent with TOPO's acting as a Lewis base. PL is abruptly and irreversibly quenched beginning at ∼10 mM, with the effect saturating at several hundred millimolar concentration. From the corresponding ^{31}P NMR and IR experiments, solution aggregation appears to onset in the 10 mM concentration regime. By use of MacroModel calculations, evidence was obtained that formation of "head-to-tail" TOPO dimers is favorable by ∼50 kJ/mol and the irreversible PL quenching signature was attributed to the ability of these species to bind at multiple surface sites and withdraw electron density from the semiconductor.

Adsorption of dialkyl sulfides, which are candidate CVD precursor molecules, has been examined on CdSe substrates by Lorenz et al.[210] Reversible PL enhancements are seen, fitting the dead-layer model, with the magnitude increasing for R_2S in the order

CH_3 < C_2H_5 < n-C_3H_7 < i-C_3H_7 < t-C_4H_9. Both electronic effects, correlated with ionization potentials, and steric effects appear to influence the PL response. Dimethyl selenide and dimethyl telluride gave similar responses to that of dimethyl sulfide.

It is worth mentioning that there is a substantial literature regarding the effects of sulfur-containing, redox-active molecules on II−VI semiconductor electrodes. These semiconductors have been used extensively in photoelectrochemical cells. Inorganic and organic sulfur-containing species have been observed to stabilize both polycrystalline and single-crystal CdS and CdSe electrodes.[211]

f. Metal Complex Adsorbates

Adsorption of a variety of lanthanide and transition metal complexes has been studied on CdS and CdSe surfaces. A series of lanthanide β-diketonate complexes [Ln(fod)$_3$, where Ln = lanthanide; fod = 6,6,7,7,8,8,8-heptafluoro-2,2-dimethyl-3,5-octanedionato anion] were adsorbed onto CdSe from isooctane solutions and caused reversible quenching, consistent with their acting as Lewis acids toward the surface.[212] Binding constants increased from left to right across the lanthanide series, paralleling the cross-period trend in lanthanide acidity. The magnitude of the PL responses appeared to correlate with contact shifts calculated for use of the lanthanide complexes as NMR shift reagents.

As described above in section IV.B, a variety of transition metal complexes have been shown to bind such molecules as oxygen and carbon monoxide when used as transducer films on semiconductor surfaces. Solution studies have been performed with several of these metal complexes both in the presence and absence of the gas with which they react and can lead to dramatically different PL adsorption responses. For example, methylene chloride solutions of *N,N′*-ethylenebis(3-methoxysalicylideneiminato)cobalt(II), which binds oxygen reversibly, produce a PL enhancement that fits the dead-layer model when the solution is nitrogen-saturated (up to a concentration of ~50 μM, whereupon irreversible quenching occurs, perhaps reflecting multilayer formation) and quenching when oxygen-saturated.[94]

Toluene solutions of Vaska's complex, *trans*-ClIr(CO)(PPh_3)$_2$, cause a PL enhancement in nitrogen-saturated solution; a larger PL enhancement in carbon monoxide-saturated solution, where only the carbonyl adduct is observed by IR spectroscopy; and a quenching of PL intensity in oxygen-saturated solution, where only the oxygen adduct is observed by IR spectroscopy.[93] The direction of the effects of carbon monoxide and oxygen on PL response in solution mimics what is observed for films of Vaska's complex deposited onto CdSe that are used for chemical sensing (see section IV.B). All of the solution and film data were fit to the dead-layer model.

The divalent metal octaethylporphyrins (OEP) and tetraphenylporphyrins (TPP) that have been studied as films were also examined in solution by Ivanisevic et al.[98] For many of these complexes, evidence was obtained that the surface mediates adduct formation with dissolved oxygen, as the PL responses were often dramatically and reversibly altered in passing from nitrogen- to oxygen-saturated methylene chloride solutions. For example, NiTPP induced substantial PL quenching in nitrogen-saturated solution and a marked enhancement in oxygen-saturated solution, relative to the solvent baseline, that had saturated by use of ~20% of the saturated oxygen concentration. Similar effects were seen for the TPP and OEP complexes of divalent Mg, Ni, and Zn. The critical role of the semiconductor surface in facilitating this interaction is underscored by the observation that there was no corresponding change in the solution electronic spectra of these compounds.

Trivalent MTPPCl complexes (M = Mn, Fe, Co) quench n-CdSe PL reversibly in nitrogen-saturated methylene chloride solution, with binding constants of approximately 10^3−10^4 M^{-1}.[100] On saturation with NO, these compounds react irreversibly to form nitrosyl adducts, which reversibly enhance the CdSe PL intensity with similar binding constants.

g. Multifunctional Adsorbates

In addition to the solution binding studies of bifunctional diamines and diphosphines noted above, binding of a family of alkanolamines and related species to CdSe has been characterized by Meeker et al.[96] As noted in section IV.B, films of these compounds can bind CO_2 reversibly as carbamates. Solution PL experiments in nitrogen-saturated THF were conducted and revealed that ethanolamine, 3-aminopropanol, and 4-aminobutanol all cause reversible PL enhancements that can be fit to either single site or multisite Langmuir adsorption isotherm models.[96] Characterization in THF solution of the binding of related molecules provided insight into some of the structural and electronic features that appear to be necessary for detection of carbon dioxide when the compounds are deposited as films onto CdSe substrates.

Adsorption of multifunctional DNA bases—adenine (A), thymine (T), cytosine (C), guanine (G)—has been studied in methanol, dimethyl sulfoxide (DMSO), and chloroform.[213] In methanol and chloroform, all four bases quench the emission from n-CdSe reversibly, while solutions of these bases in DMSO do not elicit a PL response. However, complementary base pairs (A,T and C, G) in DMSO yield modest PL quenching. These results provided evidence for surface-mediated promotion and detection of these hydrogen-bonded species.

PL changes induced by aggregate formation have also been observed in methanol and cyclohexane solutions of acrylic acid derivatives.[214] Comparison of PL and IR data indicate that surface binding leading to PL quenching involves the carboxylic acid proton. In methanol solution, the acrylic acid monomer was compared with poly(acrylic acid) (PAA) having molecular weights in the range of 2000−100000. The dependence of PL quenching on polymer concentration is independent of chain length, indicating that the same fraction of CdSe surface sites are used. Kinetic studies based on temporal PL changes indicated that adsorption was diffusion controlled.

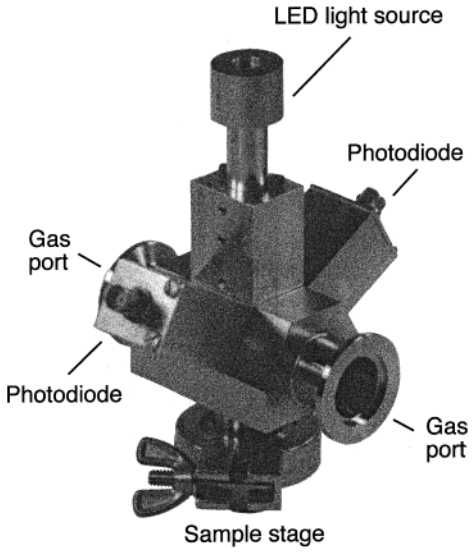

Figure 21. Hybrid sensor device employing an emissive semiconductor detection element. The unit is approximately 15 cm in height. (Reprinted from ref 188.)

VI. Applications to Chemical Sensing and Summary

As this article has attempted to show, II−VI and III−V semiconductors hold considerable promise as chemical sensor platforms in that there is now a considerable body of literature demonstrating the coupling of surface chemistry to perturbation of the solids' electrooptical properties. While many of these relationships are still largely empirical, the emergence of increasingly sophisticated analytical tools for characterization of these semiconductor-derived interfaces provides considerable opportunity for tailoring them to sensor applications. We conclude this review article by summarizing some of the opportunities and challenges associated with embodiments of sensor structures based on II−VI and III−V semiconductor materials.

An appealing feature of PL-based II−VI and III−V semiconductor sensor structures is that in their most skeletal form they need consist of nothing more than a light source, light detector, and semiconductor. An early example involved use of an $(NH_4)_2S$-passivated GaAs detector that was placed in a wastewater stream and used to detect the presence of dissolved ammonia through PL changes.[215] In principle, all three sensor components can be prepared from semiconductors, since diodes can be used for optical excitation and detection, and a semiconductor can also serve as the sensor element. Geisz and Winder built such a hybrid structure using a LED for excitation, a pair of photodiodes for detecting emitted light and reflected exciting light, and a GaAs sensor element, Figure 21.[27,188] In principle, future embodiments could be constructed from a single chip that comprises a LED or diode laser to deliver light to the semiconductor sensor surface and a photocell to detect the emitted light. All of these components could be constructed from III−V semiconductor materials, for example.

The PL changes described herein have also been incorporated into the detection system of a gas chromatograph and into a headspace analyzer by Lisensky et al.[215,216] When samples of CdS, CdS:Te, or CdSe were placed in series with a thermal conductivity detector (TCD), the semiconductor responded in parallel with the TCD to species that engaged in adduct formation. The PL response provides complementary information through the direction of the response (quenching for Lewis acids, enhancement for Lewis bases), response time (binding kinetics), and sensitivity (binding constant). Amines and carboxylic acids were among the compounds used to investigate these detector characteristics. Headspace analysis was demonstrated by placing CdSe above a sample of solid ammonium carbamate, $NH_4CO_2NH_2$.[215] As the solid was heated to produce ammonia and carbon dioxide, the PL intensity of the semiconductor increased with ammonia pressure.

Sensing need not require single-crystal samples nor PL as the detection method. Polycrystalline thin films of CdS and CdSe have been used to sense gases.[217−219] At elevated temperatures of 370−420 K, the conductivity of CdS and CdSe thin films is reduced to a percent or less of its original value upon oxygen chemisorption. The authors provide evidence that oxygen adsorbs at Cd sites, as XPS data indicate that the surface oxygen concentration increases with surface Cd concentration. Tuning the conductivity of these films by adding more surface cadmium or indium increased the sensitivity.

Key issues to be addressed in any sensing application are selectivity, long-term stability, and sensitivity. In many respects, the growth of materials by chemical vapor deposition (CVD) provides an almost ideal environment for chemical detection. Typically, flow streams consist only of a precursor gas and carrier gas, limiting the species that can elicit a response. Use of a contactless, PL-based CdSe sensor for such an environment has been reported, with a bifurcated optical fiber used to deliver the exciting light from a laser and the emitted light to a detector.[199] The concentrations of many of the gaseous analytes that have been detected using CdSe PL (section V.B), ranging typically from less than a Torr to hundreds of Torr, would be appropriate for detection in CVD flowstreams.

Multicomponent systems are more difficult to characterize, since the overall response of a single semiconductor surface will, in general, be a convolution of the individual analyte responses and their relative ability to compete for surface binding sites. The research described herein with different surface modifications is promising in this regard, because there is now considerable evidence that coatings can be used to impart selectivity toward targeted analytes. This kind of approach is relatively new, and other methodologies developed for selective sensing and for tuning sensitivity and response time—imprinted polymers, for example[220]—may be used in conjunction with II−VI and III−V transducer platforms. Arrays of small semiconductor chips that employ a range of surface modifications could be used, in principle, to characterize a mixture of analytes. Another encouraging feature of some of the

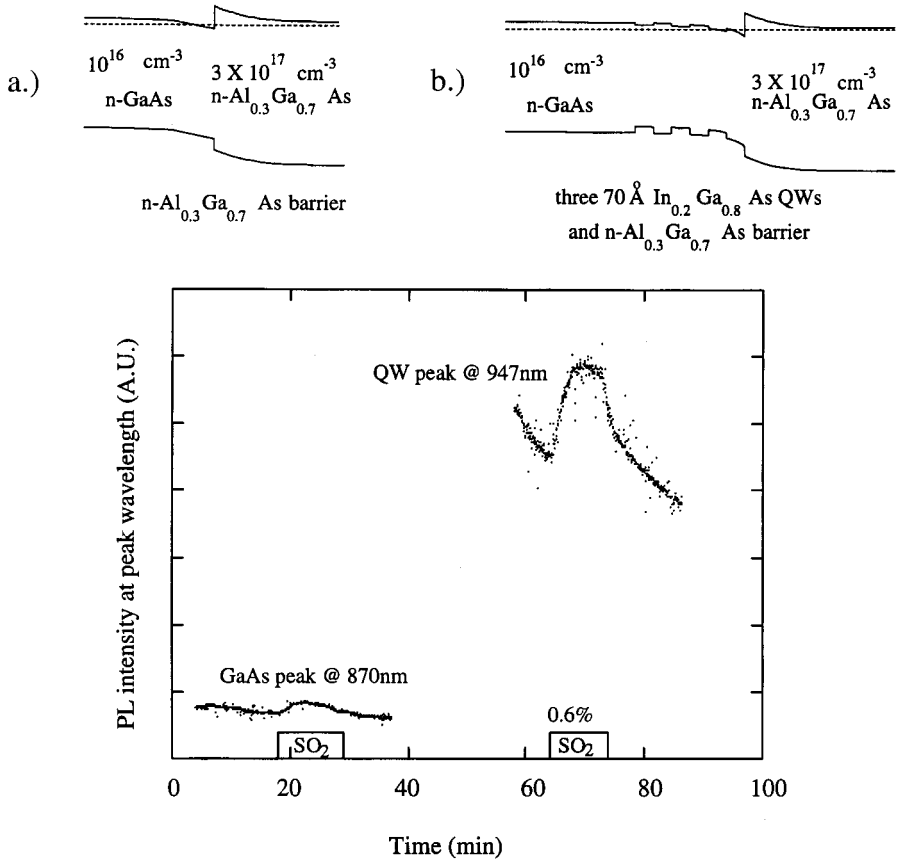

Figure 22. (Top panels) Heterostructures comprising (a) a single n-$Al_{0.3}Ga_{0.7}As$ barrier and (b) three 70 Å $In_{0.2}Ga_{0.8}As$ quantum wells and a n-$Al_{0.3}Ga_{0.7}As$ barrier. (Bottom panel) PL response to SO_2 from the GaAs layer of structure a and from the quantum wells (QW) of structure b. Both samples were excited at 458 nm at room temperature. (Reprinted from ref 27.)

surface-modified sensor structures that have thus far been reported is that in some cases they appear to be far more robust than bare etched surfaces.[94]

Finally, some discussion of tuning electronic structure from the semiconductor side of the interface as a means to optimize analyte detection is warranted. As an example, Geisz et al. used numerical modeling to design and construct heterostructures such as that shown in Figure 22 that enhance adsorbate-induced PL effects by control of carrier transport properties.[27,28] As Figure 22 shows, substantial improvements in sensitivity can be realized by this method, which can be extended to a variety of other advanced heterostructures.

In summary, while our understanding of II−VI and III−V semiconductor−molecular interfaces is still at a relatively young stage of development, it is advancing rapidly. There is reason to be optimistic that the experimental and theoretical tools that have become available for characterizing these interfaces will permit the design and construction of chemical sensors that can be used to satisfy a broad range of sensing needs.

VII. Acknowledgments

A.B.E. and T.F.K. are grateful to the National Science Foundation for support of their research on semiconductor-based chemical sensors and to their co-workers who have contributed to many of the articles described herein. We thank A. Ivanisevic, M. Khoudiakov, E. Mengelt, A.-M. Nickel, K. Nordell, C. Paulson, K. Rickert, and Professors D. Cahen, R. Hamers, F. Himpsel, and C. Landis for helpful discussions and for critically reading parts or all of this manuscript. K. Rickert is thanked for assistance with preparation of the manuscript.

VIII. References

(1) Ellis, A. B.; Brainard, R. J.; Kepler, K. D.; Moore, D. E.; Winder, E. J.; Kuech, T. F.; Lisensky, G. C. *J. Chem. Educ.* **1997**, *74*, 680−684.
(2) Ruda, H. E. *Science* **1999**, *283*, 646−647.
(3) Kruis, F. E.; Fissan, H.; Peled, A. *J. Aerosol Sci.* **1998**, *29*, 511−535.
(4) Bessolov, V. N.; Lebedev, M. V. *Semiconductors* **1998**, *32*, 1141−1156.
(5) Simpson, W. C.; Yarmoff, J. A. *Annu. Rev. Phys. Chem.* **1996**, *47*, 527−554.
(6) Bain, C. D. *Adv. Mater.* **1992**, *4*, 591−594.
(7) Spicer, W. E.; Newman, N.; Spindt, C. J.; Liliental-Weber, Z.; Weber, E. R. *J. Vac. Sci. Technol. A* **1990**, *8*, 2084−2089.
(8) Green, A. M.; Spicer, W. E. *J. Vac. Sci. Technol. A* **1993**, *11*, 1061−1069.
(9) Ertl, C.; Gerischer, H. In *Physical Chemistry: An Advanced Treatise*; Jost, W., Ed.; Academic Press: New York, 1970; Vol. 10, Chapter 7.
(10) Wolkenstein, T. *Electronic Processes on Semiconductor Surfaces During Chemisorption*; Consultants Bureau: New York, 1991.
(11) Parr, R. G.; Donnelly, R. A.; Levy, M.; Palke, W. E. *J. Chem. Phys.* **1978**, *68*, 3801−3807.
(12) Parr, R. G.; Pearson, R. G. *J. Am. Chem. Soc.* **1983**, *105*, 7512−7516.
(13) Pearson, R. G. *Proc. Natl. Acad. Sci. U.S.A.* **1986**, *83*, 8440−8441.
(14) Hoffmann, R. *Solids and Surfaces: A Chemist's View of Bonding in Extended Structures*; VCH Publishers: New York, 1988.
(15) Guo-Ping, J.; Ruda, H. E. *J. Appl. Phys.* **1996**, *79*, 3758−3762.
(16) Jiang, G. P.; Ruda, H. E. *J. Appl. Phys.* **1998**, *83*, 5880−5884.

(17) Ohno, T. *Phys. Rev. B* **1991**, *44*, 6306−6311.
(18) Ow, K. N.; Wang, X. W. *Phys. Rev. B* **1996**, *54*, 17661−17666.
(19) Sze, S. M. *Physics of Semiconductor Devices*, 2nd ed.; John Wiley & Sons: New York, 1981.
(20) Zangwill, A. *Physics at Surfaces*; Cambridge University Press: New York, 1988, 102−104.
(21) Shockley, W.; Read, W. T. *Phys. Rev.* **1952**, *87*, 835−842.
(22) Hobson, W. S.; Johnson, P. B.; Ellis, A. B.; Biefeld, R. M. *Appl. Phys. Lett.* **1984**, *45*, 150−152.
(23) Hobson, W. S.; Ellis, A. B. *J. Appl. Phys.* **1983**, *54*, 5956−5960.
(24) Hollingsworth, R. E.; Sites, J. R. *J. Appl. Phys.* **1982**, *53*, 5357−5358.
(25) Burk, A. A., Jr.; Johnson, P. B.; Hobson, W. S.; Ellis, A. B. *J. Appl. Phys.* **1986**, *59*, 1621−1626.
(26) Mettler, K. *Appl. Phys.* **1977**, *12*, 75−82.
(27) Geisz, J. F. Ph.D. Thesis, University of Wisconsin−Madison, 1995.
(28) Geisz, J. F.; Kuech, T. F.; Ellis, A. B. *J. Appl. Phys.* **1995**, *77*, 1233−1240.
(29) Ley, L.; Cardona, M.; Pollak, R. A.; Ley, L., Cardona, M., Eds.; Springer-Verlag: Berlin, 1979; Vol. 2. Photoemission in Solids. Ch. 2.
(30) Hansson, G. V.; Uhrberg, R. I. G. *Surf. Sci. Rep.* **1988**, *9*, 197−292.
(31) Woodruff, D. P. *J. Synchrotron Rad.* **1995**, *2*, 276−287.
(32) Himpsel, F. J.; Meyerson, B. S.; McFeely, F. R.; Morar, J. F.; Taleb-Ibrahimi, A.; Yarmoff, J. A.; Campagna, M., Rossi, R., Eds.; North-Holland: Amsterdam, 1990. Enrico Fermi School on Photoemission and Absorption Spectroscopy of Solids and Interfaces with Synchrotron Radiation.
(33) Sugahara, H.; Oshima, M.; Oigawa, H.; Shigekawa, H.; Nannichi, Y. *J. Appl. Phys.* **1991**, *69*, 4349−4353.
(34) Chabal, Y. J. *Surf. Sci. Rep.* **1988**, *8*, 211−357.
(35) *Spectroscopy of Surfaces*; Clark, R. J. H., Hester, R. E., Eds.; John Wiley & Sons Ltd.: New York, 1988.
(36) Ibach, H.; Mills, D. L. *Electron Energy Loss Spectroscopy and Surface Vibrations*; Academic Press: New York, 1982.
(37) *Vibrational Spectroscopy of Adsorbates*; Wills, R. F., Ed.; Springer-Verlag: Berlin, 1980.
(38) *Vibrational Spectroscopy of Molecules on Surfaces. Methods of Surface Characterization*; Yates, J. T., Madey, T. E., Eds.; Plenum Press: New York, 1987; Vol. 1.
(39) http://www.chem.qmw.ac.uk/surfaces/scc/scat5.htm (Accessed Aug 1999).
(40) Woodruff, D. P.; Bradshaw, A. M. *Rep. Prog. Phys.* **1994**, *57*, 1029−1080.
(41) Bradshaw, A. M.; Woodruff, D. P.; Eberhardt, W., Eds.; Springer-Verlag: Berlin, 1995. Applications of Synchrotron Radiation: High-Resolution Studies of Molecules and Molecular Absorbates on Surfaces. pp 127−169.
(42) Kamiya, I.; Aspnes, D. E.; Florez, L. T.; Harbison, J. P. *Phys. Rev. B* **1992**, *46*, 15894−15904.
(43) McGilp, J. F. *J. Phys. Condens. Matter.* **1990**, *2*, 7985−8006.
(44) Berkovits, V. L.; Kiselev, V. A.; Safarov, V. I. *Surf. Sci.* **1989**, *211/212*, 489−502.
(45) Chiaradia, P.; Paget, D.; Bonnet, J. E.; Martin-Gago, J.; Berkovits, V. L. *J. Appl. Phys.* **1996**, *80*, 5372−5376.
(46) http://www.chem.qmw.ac.uk/surfaces/scc/scat5_6.htm (Accessed Aug 1999).
(47) Chung, C.-H.; Yi, S. I.; Weinberg, W. H. *Appl. Phys. Lett.* **1996**, *69*, 3369−3371.
(48) Yi, S. I.; Chung, C.-H.; Weinberg, W. H. *J. Vac. Sci. Technol. A* **1997**, *15*, 1168−1172.
(49) *Procedures in Scanning Probe Microscopies*; Colton, R. J., Engel, A., Frommer, J. E., Gaub, H. E., Gewirth, A. A., Guckenberger, R., Rabe, J., Heckl, W. M., Parkinson, B., Eds.; John Wiley & Sons: Chichester, 1998.
(50) McLean, A. B.; Feenstra, R. M.; Taleb-Ibrahimi, A.; Ludeke, R. *Phys. Rev. B* **1989**, *39*, 12925−12928.
(51) Martensson, P.; Feenstra, R. M. *Phys. Rev. B* **1989**, *39*, 7744−7753.
(52) Feenstra, R. M. *Phys. Rev. Lett.* **1989**, *63*, 1412−1415.
(53) Rhoderick, E. H. *Metal-Semiconductor Contacts*; Oxford University Press: New York, 1988.
(54) Nicollian, E. H. *MOS (Metal Oxide Semiconductor) Physics and Technology*; Wiley: New York, 1982.
(55) Baikie, I. D.; Estrup, P. J. *Rec. Sci. Instrum.* **1998**, *69*, 3902−3907.
(56) Lägel, B.; Baikie, I. D.; Petermann, U. *Mater. Res. Soc. Proc.* **1998**, *501*, 619−626.
(57) Berkovits, V. L.; Ulin, V. P.; Paget, D.; Bonnet, J. E.; L'voya, T. V.; Chiaradia, P.; Lantratov, V. M. *J. Vac. Sci. Technol. A* **1998**, *16*, 2528−2538.
(58) Guerts, J. *Surf. Sci. Rep.* **1993**, *18*, 1−89.
(59) Pollak, F. H.; Shen, H. *Mater. Sci. Eng.* **1993**, *R10*, 275−374.
(60) Shen, H.; Zhou, W.; Pamulapati, J.; Ren, F. *Appl. Phys. Lett.* **1999**, *74*, 1430−1432.
(61) Railkar, T. A.; Bhide, R. S.; Bhoraskar, S. V.; Manorama, V.; Rao, V. J. *J. Appl. Phys.* **1992**, *72*, 155−157.
(62) Saitoh, T.; Hasegawa, H. *Appl. Surf. Sci.* **1992**, *56−58*, 94−99.
(63) Lunt, S. R.; Ryba, G. N.; Santangelo, P. G.; Lewis, N. S. *J. Appl. Phys.* **1991**, *70*, 7449−7467.
(64) Gottesfeld, S. *Ber. Bunsen-Ges. Phys. Chem.* **1987**, *91*, 362−369.
(65) Evenor, M.; Gottesfeld, S.; Harzion, Z.; Huppert, D.; Feldberg, S. W. *J. Phys. Chem.* **1984**, *88*, 6213−6218.
(66) Leung, L. K.; Meyer, G. J.; Lisensky, G. C.; Ellis, A. B. *J. Phys. Chem.* **1990**, *94*, 1214−1216.
(67) Benjamin, D.; Huppert, D. *J. Phys. Chem.* **1988**, *92*, 4676−4679.
(68) Kern, W. *RCA Rev.* **1978**, *39*, 278−308.
(69) Kern, W.; Deckert, C. A. In *Thin Film Processes*; Vossen, J. L., Kern, W., Eds.; Academic Press: New York, 1978.
(70) Stirland, D. J.; Straughan, B. W. *Thin Solid Films* **1976**, *31*, 139−170.
(71) McGhee, L.; McMeekin, S. G.; Nicol, I.; Robertson, M. I.; Winfield, J. M. *J. Mater. Chem.* **1994**, *4*, 29−34.
(72) Strehlow, W. H. *J. Appl. Phys.* **1969**, *40*, 2928−2932.
(73) Komisarchik, M. S.; Prokator, L. M.; Orlov, Y. F. *Inorg. Mater.* **1984**, *20*, 16−19.
(74) Komisarchik, M. S.; Novosel'tseva, T. D.; Rumyantseva, T. Y.; Lapushkina, L. V.; Orlov, F. Y. *Inorg. Mater.* **1987**, *23*, 1595−1598.
(75) Orlov, Y. F.; Komisarchik, M. S. *Russ. J. Appl. Chem.* **1995**, *68*, 1548−1550.
(76) Banerji, K. K. *Indian J. Chem.* **1973**, *11*, 244−245.
(77) Danaher, W. J.; Lyons, L. E.; Marychurch, M.; Morris, G. C. *Appl. Surf. Sci.* **1986**, *27*, 338−354.
(78) Hodes, G.; Manassen, J.; Cahen, D. *J. Electrochem. Soc.* **1981**, *128*, 2325−2330.
(79) Hickman, J. J.; Wrighton, M. S. *J. Am. Chem. Soc.* **1991**, *113*, 4440−4448.
(80) Riedinger, S. L.; Snyder, D. W.; Ko, E. I.; Sides, P. J. *Mater. Sci. Eng.* **1992**, *B15*, L9−L12.
(81) Bowen Katari, J. E.; Covin, V. L.; Alivisatos, A. P. *J. Phys. Chem.* **1994**, *98*, 4109−4117.
(82) Brillson, L. J. *Surf. Sci.* **1977**, *69*, 62−68.
(83) Kelly, J. J.; Reynders, A. C. *Appl. Surf. Sci.* **1987**, *29*, 149−164.
(84) Bryce, C.; Berk, D. *Ind. Eng. Chem. Res.* **1996**, *35*, 4464−4470.
(85) Massies, J.; Contour, J. P. *J. Appl. Phys.* **1985**, *58*, 806−810.
(86) Barycka, I.; Zuvel, I. *J. Mater. Sci.* **1987**, *22*, 1299−1304.
(87) Mori, Y.; Watanabe, N. *J. Electrochem. Soc.* **1978**, *125*, 1510−1514.
(88) Steele, M. C.; MacIver, B. A. *Appl. Phys. Lett.* **1976**, *28*, 687−688.
(89) Carpenter, M. K.; VanRyswyk, H.; Ellis, A. B. *Langmuir* **1985**, *1*, 605−607.
(90) Van Ryswyk, H.; Ellis, A. B. *J. Am. Chem. Soc.* **1986**, *108*, 2454−2555.
(91) Licht, S.; Peramunage, D. *J. Electrochem. Soc.* **1992**, *139*, L23−L26.
(92) Arent, D. J.; Hidalgoluangdilok, C.; Chun, J. K. M.; Bocarsly, A. B.; Woods, R. E. *J. Electroanal. Chem.* **1992**, *328*, 295−310.
(93) Brainard, R. J.; Ellis, A. B. *J. Phys. Chem. B* **1997**, *101*, 2533−2539.
(94) Moore, D. E.; Lisensky, G. C.; Ellis, A. B. *J. Am. Chem. Soc.* **1994**, *116*, 9487−9491.
(95) Hughes, E. W.; Wilmarth, W. K.; Calvin, M. *J. Am. Chem. Soc.* **1946**, *68*, 2273−2278.
(96) Meeker, K.; Ellis, A. B. *J. Phys. Chem. B* **1999**, *103*, 995−1001.
(97) Moore, D. E.; Meeker, K.; Ellis, A. B. *J. Am. Chem. Soc.* **1996**, *118*, 12997−13001.
(98) Ivanisevic, A.; Ellis, A. B. *J. Phys. Chem. B* **1999**, *103*, 1914−1919.
(99) Ashkenasy, G.; Ivanisevic, A.; Cohen, R.; Felder, C. E.; Cahen, D.; Ellis, A. B.; Shanzer, A. *J. Am. Chem. Soc.* **2000**, *122*, 1116−1122.
(100) Ivanisevic, A.; Reynolds, M. F.; Burstyn, J. N.; Ellis, A. B. *J. Am. Chem. Soc.* **2000**, *122*, 3731−3738.
(101) Van Vechten, J. A. *Corros. Sci.* **1990**, *31*, 39−52.
(102) Offsey, S.; Woodall, J.; Warren, A.; Kirchner, P.; Chappell, T.; Petit, G. *Appl. Phys. Lett.* **1986**, *48*, 475−477.
(103) Hirota, Y.; Homma, Y.; Sugii, K. *Appl. Phys. Lett.* **1991**, *58*, 2794−2796.
(104) Ives, N. A.; Stupian, G. W.; Leung, M. S. *Appl. Phys. Lett.* **1987**, *50*, 256−258.
(105) Chambers, S. A.; Sundaram, V. S. *J. Vac. Sci. Technol. B* **1991**, *9*, 2256−2262.
(106) Ferrari, L.; Fodonipi, M.; Righini, M.; Selci, S. *Surf. Sci.* **1995**, *331−333*, 447−452.
(107) Hasegawa, H.; Ishii, H.; Sawada, T.; Saitoh, T.; Konishi, S.; Liu, Y.; Ohno, H. *J. Vac. Sci. Technol. B* **1988**, *6*, 1184−1192.
(108) Hasegawa, H.; Saitoh, T.; Konishi, S.; Ishi, H.; Ohno, H. *Jpn. J. Appl. Phys.* **1988**, *27*, L2177−L2179.
(109) Fan, J.-F.; Oigawa, H.; Nannichi, Y. *Jpn. J. Appl. Phys.* **1988**, *27*, L1331−L1333.
(110) Hildebrandt, S.; Schreiber, J.; Kircher, W.; Kuzmendo, R. *Appl. Surf. Sci.* **1993**, *63*, 153−157.
(111) Lu, Z. H.; Graham, M. J. *Phys. Rev. B* **1993**, *48*, 4604−4607.

(112) Lunt, S. R.; Santangelo, P. G.; Lewis, N. S. *J. Vac. Sci. Technol. B* **1991**, *9*, 2333−2336.
(113) Sandroff, C. J.; Hegde, M. S.; Chang, C. C. *J. Vac. Sci. Technol. B* **1989**, *7*, 841−844.
(114) Sandroff, C. J.; Hegde, M. S.; Farrow, L. A.; Chang, C. C.; Harbison, J. P. *Appl. Phys. Lett.* **1989**, *54*, 362−364.
(115) Spindt, C. J.; Liu, D.; Miyano, K.; Meissner, P. L.; Chiang, T.; Kendelewicz, T.; Lindau, I.; Spicer, W. E. *Appl. Phys. Lett.* **1989**, *55*, 861−863.
(116) Oigawa, H.; Fan, J.-F.; Nannichi, Y.; Ando, K.; Saiki, K.; Koma, A. *Jpn. J. App. Phys.* **1989**, *28*, L340−L342.
(117) Wang, X.-S.; Weinberg, W. H. *J. Appl. Phys.* **1994**, *75*, 2715−2717.
(118) Hirayama, H.; Matsumoto, Y.; Oigawa, H.; Nannichi, Y. *Appl. Phys. Lett.* **1989**, *54*, 2565−2567.
(119) Moriarty, P.; Murphy, B.; Roberts, L.; Cafolla, A. A.; Hughes, G.; Koenders, L.; Bailey, P. *Phys. Rev. B* **1994**, *50*, 14237−14245.
(120) Ke, Y.; Milano, S.; Wang, X. W.; Tao, N.; Darici, Y. *Surf. Sci.* **1998**, *415*, 29−36.
(121) Tsukamoto, S.; Koguchi, N. *Appl. Phys. Lett.* **1994**, *65*, 2199−2201.
(122) Sugiyama, M.; Maeyama, S. *Surf. Sci.* **1997**, *385*, L911−L916.
(123) Sugiyama, M.; Maeyama, S.; Oshima, M. *Phys. Rev. B* **1994**, *50*, 4905−4908.
(124) Gu, G. Y.; Ogryzlo, E. A.; Wong, P. C.; Zhou, M. Y.; Mitchell, K. A. R. *J. Appl. Phys.* **1992**, *72*, 762−765.
(125) Tiedje, T.; Colbow, K. M.; Rogers, D.; Fu, Z.; Eberhardt, W. *J. Vac. Sci. Technol. B* **1989**, *7*, 837−840.
(126) Lu, Z. H.; Graham, M. J.; Feng, X. H.; Yang, B. X. *Appl. Phys. Lett.* **1993**, *62*, 2932−2934.
(127) Berkovits, V. L.; Paget, D. *Appl. Phys. Lett.* **1992**, *61*, 1835−1837.
(128) Paget, D.; Bonnet, J. E.; Berkovits, V. L.; Chiaradia, P.; Avila, J. *Phys. Rev. B* **1996**, *53*, 4604−4614.
(129) Medvedev, Y. V. *Appl. Phys. Lett.* **1994**, *64*, 3458−3460.
(130) Ohno, T.; Shiraishi, K. *Phys. Rev. B* **1990**, *42*, 11194−11197.
(131) Shimoda, M.; Tsukamoto, S.; Koguchi, N. *Surf. Sci.* **1998**, *395*, 75−81.
(132) Shimoda, M.; Tsukamoto, S.; Koguchi, N. *Surf. Sci.* **1998**, *402−404*, 669−672.
(133) Oigawa, H.; Fan, J.-F.; Nannichi, Y.; Ando, K.; Sugahara, H.; Oshima, M. *Jpn. J. Appl. Phys.* **1991**, *30*, L322−L325.
(134) Xia, H.; Lennard, W. N.; Massoumi, G. R.; van Eck, J. J. J.; Huang, L. J.; Lau, W. M.; Landheer, D. *Surf. Sci.* **1995**, *324*, 159−168.
(135) Patrin, J., C.; Li, Y. Z.; Chander, M.; Weaver, J. H. *Appl. Phys. Lett.* **1993**, *62*, 1277−1279.
(136) Patrin, J. C.; Weaver, J. H. *Phys. Rev. B* **1993**, *48*, 17913−17921.
(137) Liu, Y.; Komrowski, A. J.; Kummel, A. C. *Phys. Rev. Lett.* **1998**, *81*, 413−416.
(138) Jacobi, K.; Steinert, G.; Ranke, W. *Surf. Sci.* **1976**, *57*, 571−579.
(139) Singh, N. K.; Bolzan, A.; Foord, J. S.; Wright, H. *Surf. Sci.* **1998**, *409*, 272−282.
(140) Lasky, P. J.; Lu, P. H.; Luo, Y.; Slater, D. A.; Osgood, R. M., Jr. *Surf. Sci.* **1996**, *364*, 312−324.
(141) Lam, H. T.; Venkateswaran, N.; Vohs, J. M. *Surf. Sci.* **1998**, *401*, 34−36.
(142) Venkateswaran, N.; Roe, C. L.; Lam, H.-T.; Vohs, J. M. *Surf. Sci.* **1996**, *365*, 125−135.
(143) Vogt, K. W.; Kohl, P. A.; Abys, J. A. *AIChE J.* **1995**, *41*, 2282−2291.
(144) Soukiassian, P.; Starnberg, H. I.; Kendelewicz, T.; Hurych, Z. D. *Phys. Rev. B* **1990**, *42*, 3769−3772.
(145) Sheen, C. W.; Shi, J. X.; Martensson, J.; Parikh, A. N.; Allara, D. L. *J. Am. Chem. Soc.* **1992**, *114*, 1514−1515.
(146) Nakagawa, O. S.; Ashok, S.; Sheen, C. W.; Martensson, J.; Allara, D. L. *Jpn. J. Appl. Phys. Part 1* **1991**, *30*, 3759−3762.
(147) Yang, H. C.; Dermody, D. L.; Xu, C.; Ricco, A. J.; Crooks, R. M. *Langmuir* **1996**, *12*, 726−735.
(148) Tabib-Azar, M.; Dewa, A. S.; Ko, W. H. *Appl. Phys. Lett.* **1988**, *52*, 206−208.
(149) Rao, V. J.; Kulkarni, V. S. *Thin Solid Films* **1991**, *198*, 357−362.
(150) Shimanoe, K.; Sakashita, M. *Jpn. J. Appl. Phys. Part 1* **1993**, *32*, 1064−1067.
(151) Xue, Q.; Ling, Y.; Ogino, T.; Sakata, T.; Hasegawa, Y.; Hashizume, T.; Shinohara, H.; Sakurai, T. *Thin Solid Films* **1996**, *281−282*, 618−623.
(152) Leung, L. K.; Komplin, N. J.; Ellis, A. B.; Tabatabaie, N. *J. Phys. Chem.* **1991**, *95*, 5918−5924.
(153) Keys, A.; Simon, G. B.; Barron, A. R. *Polyhedron* **1998**, *17*, 3121−3130.
(154) Spindt, C. J.; Besser, R. S.; Cao, R.; Miyano, K.; Helms, C. R.; Spicer, W. E. *J. Vac. Sci. Technol. A* **1989**, *7*, 2466−2468.
(155) Besser, R. S.; Helms, C. R. *Appl. Phys. Lett.* **1988**, *52*, 1707−1709.
(156) Paget, D.; Gusev, A. O.; Berkovits, V. L. *Phys. Rev. B* **1996**, *53*, 4615−4622.
(157) Liu, D.; Zhang, T.; LaRue, R. A.; Harris, J. S., Jr.; Sigmon, T. W. *Appl. Phys. Lett.* **1988**, *53*, 1059−1061.
(158) Arens, M.; Kinsky, J.; Richter, W.; Eberl, K. *Surf. Sci.* **1996**, *352−354*, 740−744.
(159) Yablonovitch, E.; Skromme, B. J.; Bhat, R.; Harbison, J. P.; Gmitter, T. J. *Appl. Phys. Lett.* **1989**, *54*, 555−557.
(160) Fan, J.-F.; Oigawa, H.; Nannichi, Y. *Jpn. J. Appl. Phys.* **1988**, *27*, L2125−L2127.
(161) Bessolov, V. N.; Konenkova, E. V.; Lebedev, M. V. *J. Vac. Sci. Technol. B* **1996**, *14*, 2761−2766.
(162) Bessolov, V. N.; Ivankov, A. F.; Lebedev, M. V. *J. Vac. Sci. Technol. B* **1995**, *13*, 1018−1023.
(163) Bessolov, V. N.; Ershov, S. G.; Ivankov, A. F.; Lebedev, M. V. *Phys. Solid State* **1994**, *36*, 1912−1914.
(164) Bessolov, V. N.; Ivankov, A. F.; Lebedev, M. V. *Phys. Solid State* **1996**, *38*, 308−314.
(165) Bessolov, V. N.; Lebedev, M. V.; Ivankov, A. F.; Bauhofer, W.; Zahn, D. R. T. *Appl. Surf. Sci.* **1998**, *133*, 17−22.
(166) Tabib-Azar, M.; Kang, S.; MacInnes, A. N.; Power, M. B.; Barron, A. R.; Jenkins, P. P.; Hepp, A. F. *Appl. Phys. Lett.* **1993**, *63*, 625−627.
(167) Hou, T.; Greenlief, C. M.; Keller, S. W.; Nelen, L.; Kauffman, J. F. *Chem. Mater.* **1997**, *9*, 3181−3186.
(168) Dorsten, J. F.; Maslar, J. E.; Bohn, P. W. *Appl. Phys. Lett.* **1995**, *66*, 1755−1757.
(169) Remashan, K.; Bhat, K. N. *Thin Solid Films* **1999**, *342*, 20−29.
(170) Asai, K.; Miyashita, T.; Ishigure, K.; Fukatsu, S. *J. Appl. Phys.* **1995**, *77*, 1582−1586.
(171) Bastide, S.; Butruille, R.; Cahen, D.; Dutta, A.; Libman, J.; Shanzer, A.; Sun, L.; Vilan, A. *J. Phys. Chem. B* **1997**, *101*, 2678−2684.
(172) Sandroff, C. J.; Hegde, M. S.; Farrow, L. A.; Bhat, R.; Harbison, J. P.; Chang, C. C. *J. Appl. Phys.* **1990**, *67*, 586−588.
(173) Pashley, M. D.; Li, D. *J. Vac. Sci. Technol. A* **1994**, *12*, 1848−1854.
(174) Chambers, S. A.; Sundaram, V. S. *Appl. Phys. Lett.* **1990**, *57*, 2342−2344.
(175) Scimeca, T.; Watanabe, Y.; Maeda, F.; Berrigan, R.; Oshima, M. *Appl. Phys. Lett.* **1993**, *62*, 1667−1669.
(176) Scimeca, T.; Watanabe, Y.; Berrigan, R.; Oshima, M. *Phys. Rev. B* **1992**, *46*, 10201−10206.
(177) Scimeca, T.; Watanabe, Y.; Maeda, F.; Berrigan, R.; Oshima, M. *J. Vac. Sci. Technol. B* **1994**, *12*, 3090−3094.
(178) Takatani, S.; Kikawa, T.; Nakazawa, M. *Phys. Rev. B* **1992**, *45*, 8498−8505.
(179) Kuruvilla, B. A.; Ghaisas, S. V.; Datta, A.; Banerjee, S.; Kulkarni, S. K. *J. Appl. Phys.* **1993**, *73*, 4384−4387.
(180) Kuruvilla, B. A.; Datta, A.; Shekhawat, G. S.; Sharma, A. K.; Vyas, P. D.; Gupta, R. P.; Kulkarni, S. K. *J. Appl. Phys.* **1996**, *80*, 6274−6278.
(181) Kuruvilla, B. A.; Datta, A.; Shekhawat, G. S.; Sharma, A. K.; Vyas, P. D.; Gupta, R. P.; Kulkarni, S. K. *Appl. Phys. Lett.* **1996**, *69*, 415−417.
(182) Nozaki, S.; Tamura, S.; Takahashi, K. *J. Vac. Sci. Technol. B* **1995**, *13*, 297−304.
(183) Tsuchiya, K.; Sakata, M.; Funyu, A.; Ikoma, H. *Jpn. J. Appl. Phys.* **1995**, *34*, 5926−5932.
(184) Sun, J. X.; Seo, D. J.; O'Brien, W. L.; Himpsel, F. J.; Ellis, A. B.; Kuech, T. F. *J. Appl. Phys.* **1999**, *85*, 969−977.
(185) Xu, H.; Belkouch, S.; Aktik, C.; Rasmussen, W. *Appl. Phys. Lett.* **1995**, *66*, 2125−2127.
(186) Meyer, G. J.; Lisensky, G. C.; Ellis, A. B. *J. Am. Chem. Soc.* **1988**, *110*, 4914−4918.
(187) Rives, A. B. *Langmuir* **1993**, *9*, 177−185.
(188) Winder, E. J. Ph.D. Thesis, University of Wisconsin−Madison, 1997.
(189) Atkins, P. W. *Physical Chemistry*, 6th ed.; W. H. Freeman and Co.: New York, 1998.
(190) Lisensky, G. C.; Penn, R. L.; Murphy, C. J.; Ellis, A. B. *Science* **1990**, *248*, 840−843.
(191) Kepler, K. D.; Lisensky, G. C.; Patel, M.; Sigworth, A.; Ellis, A. B. *J. Phys. Chem.* **1995**, *99*, 16011−16017.
(192) Zhang, J. Z.; Ellis, A. B. *J. Phys. Chem.* **1992**, *96*, 2700−2704.
(193) Zhang, J. Z.; Geselbracht, M. J.; Ellis, A. B. *J. Am. Chem. Soc.* **1993**, *115*, 7789−7793.
(194) Neu, D. R.; Olson, J. A.; Ellis, A. B. *J. Phys. Chem.* **1993**, *97*, 5713−5716.
(195) Winder, E. J.; Kuech, T. F.; Ellis, A. B. *J. Electrochem. Soc.* **1998**, *145*, 2475−2479.
(196) Meyer, G. J.; Leung, L. K.; Yu, J. C.; Lisensky, G. C.; Ellis, A. B. *J. Am. Chem. Soc.* **1989**, *111*, 5146−5148.
(197) Dollard, W. J.; Shumaker, M. L.; Waldeck, D. H. *J. Phys. Chem.* **1993**, *97*, 4141−4148.
(198) Brainard, R. J.; Paulson, C. A.; Saulys, D.; Gaines, D. F.; Kuech, T. F.; Ellis, A. B. *J. Phys. Chem. B* **1997**, *101*, 11180−11184.
(199) Winder, E. J.; Moore, D. E.; Neu, D. R.; Ellis, A. B.; Geisz, J. F.; Kuech, T. F. *J. Cryst. Growth* **1995**, *148*, 63−69.
(200) Murphy, C. J.; Lisensky, G. C.; Leung, L. K.; Kowach, G. R.; Ellis, A. B. *J. Am. Chem. Soc.* **1990**, *112*, 8344−8348.

(201) Bruening, M.; Moons, E.; Cahen, D.; Shanzer, A. *J. Phys. Chem.* **1995**, *99*, 8368−8373.
(202) Murphy, C. J.; Ellis, A. B. *Polyhedron* **1990**, *9*, 1913−1919.
(203) Bruening, M.; Moons, E.; Yaron-Marcovich, D.; Cahen, D.; Libman, J.; Shanzer, A. *J. Am. Chem. Soc.* **1994**, *116*, 2972−2977.
(204) Cohen, R.; Bastide, S.; Cahen, D.; Libman, J.; Shanzer, A.; Rosenwaks, J. *Adv. Mater.* **1997**, *9*, 746−749.
(205) Cohen, R.; Kronik, L.; Shanzer, A.; Cahen, D.; Liu, A.; Rosenwaks, Y.; Lorenz, J. K.; Ellis, A. B. *J. Am. Chem. Soc.* **1999**, *121*, 10545−10553.
(206) Cohen, R.; Kronik, L.; Vilan, A.; Shanzer, A.; Cahen, D. *Adv. Mater.* **2000**, *12*, 33−37.
(207) Vilan, A.; Ussyshkin, R.; Gartsman, K.; Cahen, D.; Naaman, R.; Shanzer, A. *J. Phys. Chem. B* **1998**, *102*, 3307−3309.
(208) Kadyshevitch, A.; Naaman, R.; Cohen, R.; Cahen, D.; Libman, J.; Shanzer, A. *J. Phys. Chem. B* **1997**, *101*, 4085−4089.
(209) Lorenz, J. K.; Ellis, A. B. *J. Am. Chem. Soc.* **1998**, *120*, 10970−10975.
(210) Lorenz, J. K.; Kuech, T. F.; Ellis, A. B. *Langmuir* **1998**, *14*, 1680−1683.
(211) Tan, M. X.; Laibinis, P. E.; Nguyen, S. T.; Kesselman, J. M.; Stanton, C. E.; Lewis, N. S.; John Wiley & Sons: New York, 1994; Vol. 41.
(212) Murphy, C. J.; Ellis, A. B. *J. Phys. Chem.* **1990**, *94*, 3082−3085.
(213) Meeker, K.; Ellis, A. B. *J. Phys. Chem. B* **2000**, *104*, 2500−2505.
(214) Seker, F.; Ellis, A. B. *Macromolecules* **2000**, *33*, 582−589.
(215) Luebker, E. R. M.; Leung, L. K.; Murphy, C. J.; Lisensky, G. C.; Ellis, A. B. In *Biotechnology: Bridging Research and Applications*; Kamely, D., Chakrabarty, A. M., Kornguth, S. E., Eds.; Kluwer Academic Publishers: Boston, 1991; Chapter 7.
(216) Lisensky, G. C.; Meyer, G. J.; Ellis, A. B. *Anal. Chem.* **1988**, *60*, 2531−2534.
(217) Golovanov, V.; Smyntyna, V.; Mattogno, G.; Kaciulis, S. A. *Sens. Actuators B* **1995**, *26−27*, 108−112.
(218) Smyntyna, V.; Golovanov, V.; Kaciulis, S.; Mattogno, G.; Righini, G. *Sens. Actuators B* **1995**, *24−25*, 628−630.
(219) Smyntyna, V.; Gerasutenko, V.; Golovanov, V.; Kaciulis, S.; Mattogno, G.; Viticoli, S. *Sens. Actuators B* **1994**, *22*, 189−194.
(220) Mosbach, K. *Chem. Rev.* **2000**, 0000.

CR980093R